




# Poly( $\alpha$ -methyl styrene) polymer additive for organic thin film transistors

Ziyang Zhang<sup>1</sup>, Kyeiwaa Asare-Yeboah<sup>2</sup>, Sheng Bi<sup>3,\*</sup>, and Zhengran He<sup>4,\*</sup> 

<sup>1</sup>Department of Electrical Engineering, Columbia University, New York, NY 10027, USA

<sup>2</sup>Department of Electrical and Computer Engineering, Penn State Behrend, Erie, PA 16563, USA

<sup>3</sup>Key Laboratory for Precision and Non-Traditional Machining Technology of the Ministry of Education, Dalian University of Technology, Dalian 116024, Liaoning, China

<sup>4</sup>Department of Electrical and Computer Engineering, The University of Alabama, Tuscaloosa, AL 35487, USA

**Received:** 15 September 2021

**Accepted:** 10 December 2021

**Published online:**

5 January 2022

© The Author(s), under exclusive licence to Springer Science+Business Media, LLC, part of Springer Nature 2022

## ABSTRACT

While great progress has been achieved in the research of various solution-processed organic semiconductors, the randomized crystal orientations and charge carrier mobility variations have posed tremendous challenges to implement the organic semiconductors for organic electronic device applications. Among the miscellaneous polymer additives reported to tune the crystal growth and modulate charge transport, poly( $\alpha$ -methyl styrene) (P $\alpha$ MS) has been extensively studied for its capability to improve semiconductor crystallization, reduce bulk crystal misorientation, induce phase segregation, enhance morphological uniformity and boost electrical performance of organic thin film transistors and organic electronic devices. In the first section of this article, we review the recent progress of organic electronics and highlight the crystal misorientation and mobility variation as the challenges that need to be overcome. Then, the various merits from mixing polymeric additives with organic semiconductors are discussed. In the second section, we provide an overview of the previous works that employ P $\alpha$ MS for regulating the crystal orientation alignment and modulating charge transport of miscellaneous solution-processed small-molecular organic semiconductors including 6,13-bis(triisopropylsilylethynyl) pentacene (TIPS pentacene) and 2,8-difluoro-5,11-bis(triethylsilylethynyl)anthradithiophene (diF-TESADT). By discussing these important examples, we intend to demonstrate that P $\alpha$ MS can be versatily implemented to improve other new organic semiconductor crystallization and mobility for high-performance organic electronic applications.

Address correspondence to E-mail: bish@dlut.edu.cn; zhe3@crimson.ua.edu

## 1 Introduction and background

In spite of the fast development of solution-processable organic semiconductors, the randomized crystal orientation and charge carrier mobility variations have posed technical challenges to implement the organic semiconductors in organic electronic device fabrication and application. In this section, we first provide an overview of the recent advances of the organic electronics field and highlight the cause and effect of anisotropic charge transport in organic semiconductors. Then, we discuss the various merits of mixing organic semiconductors with the general polymeric additives, which has a significant influence on controlling semiconductor crystallization and enhancing electrical charge carrier transport.

### 1.1 Recent progress in organic electronics

In recent years, major advances have been demonstrated in the development of organic electronics [1–9]. Various solution-processable organic semiconductors have been reported that exhibit improved solubility in organic solvents [10, 11], large charge carrier mobilities [12–14] and good air stability [15, 16]. Here we discuss the development and application of 6,13-bis(triisopropylsilylethynyl) pentacene (TIPS pentacene) as benchmark examples to shed lights on the recent progress of organic semiconductors and organic electronics devices [17–24]. TIPS pentacene is a p-type organic semiconductor which was originally reported in a series of studies by Anthony et al. as a derivative of pentacene [25–27]. The attachment of the bulky side groups to the backbones disrupts the herringbone packing motif and allows TIPS pentacene to dissolve in a variety of solvents [28–32]. Chen et al. reported that TIPS pentacene can find decent solubility in various organic solvents by comparing the solubility parameters of TIPS pentacene and the solvents [27]. TIPS pentacene has a solubility parameter of  $\delta = 18\text{--}19 \text{ MPa}^{1/2}$ . In order for TIPS pentacene to well dissolve in an organic solvent, the solubility parameter of the solvents must be close to that of TIPS pentacene. Thereby, chloroform ( $\delta = 19 \text{ MPa}^{1/2}$ ), tetrahydrofuran ( $\delta = 18.6 \text{ MPa}^{1/2}$ ) and toluene ( $\delta = 18.2 \text{ MPa}^{1/2}$ ) were considered to be “good solvent” for TIPS pentacene based on this criterion. Kim et al. reported a binary solvent method to grow TIPS pentacene microribbon crystals [33]. The binary solvent

comprised toluene as the main solvent and acetonitrile as the additive solvent. Microribbon crystals were formed as a result of the solvent exchange process by injecting the TIPS pentacene/toluene solution into acetonitrile, yielding an enhanced hole mobility of  $1.42 \text{ cm}^2/\text{V s}$ .

In addition, the bulky side group of TIPS pentacene is pushed away from the backbones as a result of the carbon–carbon triple bonds, giving rise to face-to-face interaction ( $\pi\text{--}\pi$  stacking) in TIPS pentacene [34–36]. The  $\pi\text{--}\pi$  stacking in TIPS pentacene molecules greatly enhances charge transport as compared to pentacene [37]. For example, Lee et al. studied the crystallization modes of TIPS pentacene by optimizing the spin coating time and reported a hole mobility of  $1.3 \text{ cm}^2/\text{V s}$  from TIPS pentacene spherulites due to the large grain size and crystal perfection [38]. Kim et al. reported a blade coating method to grow highly oriented TIPS pentacene crystals, yielding a mobility of  $1.74 \text{ cm}^2/\text{V s}$  [39]. Wang et al. optimized the dielectric surface and reported a mobility of  $2.26 \text{ cm}^2/\text{V s}$  from TIPS pentacene microwires when the polar and dispersive components of surface energy matched those of the semiconductor [40]. Bharti et al. reported a mobility of  $2.6 \text{ cm}^2/\text{V s}$  from phase segregated TIPS pentacene and polystyrene (PS) blends due to improved quality of charge transport interface [41]. Rocha et al. developed a solution shearing method to grow ordered TIPS pentacene crystals and reported a high mobility of  $6.7 \text{ cm}^2/\text{V s}$  [42]. Diao et al. reported a fluid-enhanced crystal engineering (FLUENCE) technique to control the morphological features of solution-printed TIPS pentacene thin films [43]. The recirculation in the ink induced by the micropillar-patterned printing blade effectively enhanced the crystal nucleation and growth. The FLUENCE technique gave rise to highly aligned TIPS pentacene ribbons with width and length in millimeter and centimeter scale, respectively, producing a hole mobility of  $11 \text{ cm}^2/\text{V s}$ . Su et al. reported a zone casting method to uniaxially achieve crystal alignment of TIPS pentacene crystalline arrays [44]. Zone casting TIPS pentacene in a solvent with a low boiling point and a large casting speed was found to favor the formation of aligned crystal ribbons, yielding a mobility of  $0.67 \text{ cm}^2/\text{V s}$ . Kim et al. reported a “confined evaporative capillary flow (CEC)” method to develop TIPS pentacene ribbon-shaped crystals [45]. The CEC method modulated the solution evaporation, reduced the contact line pinning and

controlled the outward hydrodynamic flow, giving rise to crystal ribbons with enlarged grain width and length. The crystal ribbons exhibited preferential crystal orientation and enhanced charge transport in a lateral direction, leading to an improved mobility of  $0.72 \text{ cm}^2/\text{V s}$ .

In addition to TIPS pentacene, other organic semiconductors have been reported with even higher mobilities by combining polymer additives and external forces. For instance, Shen et al. reported the optimization of 2,7-dioctyl[1]benzothieno[3,2-b][1]benzothiophene ( $C_8$ -BTBT)/PS phase segregation and crystallization by tuning the spin coating speed and PS weight ratio [46]. The vertically segregated  $C_8$ -BTBT was observed to crystallize at the interface between the active layer and air, giving rise to a mobility of  $6.8 \text{ cm}^2/\text{V s}$ . Haase et al. reported a solution shearing based coating method to grow  $C_8$ -BTBT [47]. By mixing  $C_8$ -BTBT with the polymer additive PS, the shearing-deposited active layer yielded a high mobility of  $12 \text{ cm}^2/\text{V s}$ . Panidi et al. reported an admixing approach of the molecular Lewis acid  $B(C_6F_5)_3$  in 2,8-difluoro-5,11-bis(triethylsilylethynyl)anthradithiophene (diF-*TESADT*) formulation before solution deposition to enhance its charge transport [48]. diF-*TESADT*/PTAA blends based on  $B(C_6F_5)_3$  showed an enhanced mobility of  $8 \text{ cm}^2/\text{V s}$ . Zhang et al. reported a mixed solvent system with blade coating to deposit pinhole free diF-*TESADT* semiconductor film with enhanced uniformity [49]. The resultant ultra-thin diF-*TESADT* film showed improved crystallinity and a mobility of  $5.54 \text{ cm}^2/\text{V s}$ .

The improved solubility in organic solvents and high charge carrier mobilities has attracted considerable attention to implement the organic semiconductors in various high performance organic electronic device applications, including organic thin film transistors [50, 51], gas sensors [52, 53], phototransistors [54–56], photodetectors [57, 58] and complementary inverters [59, 60]. For instance, gas sensors incorporating the organic semiconductors have the capability to detect the traces of gases by characterizing the fluctuation of saturation currents as a result of the gas diffusion into the transistor channel and absorption into the interfacial traps [61]. Zhuang et al. reported an off-center spin coating method to grow TIPS pentacene nanofibrillar structures as the active layer of nitrogen dioxide ( $\text{NO}_2$ ) gas sensor [53]. Gas responsivity 30 ppm  $\text{NO}_2$  was

enhanced by 221.5% by using this coating method. The organic thin film transistor based photodetectors are able to characterize the photo-to-dark current ratio from exposure with incident light of different wavelengths [62]. Benavides et al. reported the utilization of TIPS pentacene as an interlayer to decrease the dark current of poly-3-hexyl-thiophene (P3HT) and [6, 6]-phenyl c(61) butyric acid methyl ester (PCBM) based photodetector [57]. Inserting TIPS pentacene interlayer also improved the detectivity and dynamic range of the photodetector. Furthermore, the fabrication of both a p-type and n-type thin film transistor on the same substrate gives rise to complementary inverters [63, 64]. Kim et al. demonstrated a vertical stacking structure for complementary inverters comprising an n-type PCBM and p-type TIPS pentacene [65]. The n-channel and p-channel transistor showed a mobility of  $0.004 \text{ cm}^2/\text{V s}$  and  $0.25 \text{ cm}^2/\text{V s}$ , respectively, giving rise to a gain value of  $-24 \text{ V/V}$  for the inverter. These organic electronic devices can further find applications in a variety of fields such as display electronics [66], biomedical analysis [67] and pharmaceutical industry [68].

## 1.2 Random charge transport in organic semiconductors

Despite these advancements, a few significant challenges holding back the future development and application of the organic semiconductors include the randomized patterns of semiconductor crystallization in solution, mobility variation, thermal cracks caused by high deposition temperature, and effects from solvents [69–71]. For example, when the organic semiconductor TIPS pentacene is deposited by using the drop casting method, the semiconductor shows a dendritic motif of crystal growth [72, 73]. Chen et al. designed a deposition system to systematically control the crystal orientations of TIPS pentacene and correlated the crystal orientation to the charge carrier mobilities of TIPS pentacene based organic thin film transistors [74]. This research indicated that as the crystals were formed in a parallel direction with the source and drain contact electrodes, the transistors exhibited a mobility 10 times higher than that obtained from the counterparts with crystals deposited in a perpendicular direction. A similar study conducted by Akkerman et al. showed that the misoriented TIPS pentacene crystals can cause a

much larger variation in charge carrier mobility of up to a 50-fold difference [75]. In addition to TIPS pentacene, the correlation between crystal misorientations and mobility variations has also been observed in solution-based drop casting of 5,6,11,12-tetrachlorotetracene [76] and 2,5-di-(2-ethylhexyl)-3,6-bis(5'-*n*-hexyl-2,2',5',2'')terthiophen-5-yl)-pyrrolo[3,4-*c*] pyrrole-1,4-dione (SMDPPEH) [77, 78], 6,13-bis(triethylsilylethynyl) pentacene (TES pentacene) [79] and C<sub>8</sub>-BTBT [80] organic semiconductors. James et al. reported the random charge transport in TES pentacene organic crystals with different morphologies [79]. By using a zone casting method, the TES pentacene crystals were intentionally aligned with various orientations with the channel direction. The ratio of "parallel mobility" to "perpendicular mobility", which refers to the mobility measured when crystal is parallel with and perpendicular to the channel, respectively, was employed as a mobility anisotropy parameter. A mobility anisotropy parameter of 5 was measured from the TES pentacene broad domain film, whereas a much higher parameter of 21–47 was obtained from the elongated TES pentacene ribbons. Li et al. reported the random charge transport in C<sub>8</sub>-BTBT plate-like crystals with different crystal size [80]. Tuning the concentrations of both C<sub>8</sub>-BTBT semiconductor and the polymethyl methacrylate (PMMA) additive gave rise to different crystal size. Enlarged crystal size was observed to yield improved mobility uniformity, which was attributed to the reduced crystal orientation and alignment variations. These important results necessitated the homogeneous alignment of the organic semiconductor crystal orientation.

Besides randomized crystallization, deposition temperature and solvents can also pose challenges on the processing of organic semiconductors. When the substrate is heated to an elevated deposition temperature in order to promote the crystallization and alignment of the organic semiconductor [81], heating has been reported to cause thermal cracks and induce a blocking effect on charge transport [31]. Different solvent choices can impact the organic semiconductor dissolving, nucleation, crystallization, morphology, crystallinity, and charge transport. Hansen's solubility theory can usefully help determine the solvent affinity for the organic semiconductor. Hansen's solubility parameters determine the extent of mismatch between the solvent and semiconductor, which is shown by the following equation:

$$R = \sqrt{\Delta\delta_p^2 + \Delta\delta_d^2 + \Delta\delta_h^2} \quad (1)$$

In Eq. (1),  $\delta_p$ ,  $\delta_d$ , and  $\delta_h$  is the polar, dispersive and hydrogen bonding part of the intermolecularly interacting force [82, 83]. Good solubility in the solvent can be expected based on similar Hansen's solubility parameters.

### 1.3 Merits of polymer additives in controlling organic crystal growth

Polymeric additives have been demonstrated with multi-fold benefits on the crystal growth and charge transport of organic semiconductors. In this section, we will briefly discuss these benefits including improving morphology uniformity, reducing crystal misorientation, enlarging grain width, enhancing electrical stability, inducing phase segregation, and improving charge transport.

#### 1.3.1 Improving morphology uniformity

The blending of polymeric additives with organic semiconductors can not only improve the thin film morphology uniformity but also reduce the crystal misorientation [84–87]. Still taking TIPS pentacene as an example, the concept of crystal misorientation angle is introduced to better characterize the different crystal orientations on a large scale. The crystal misorientation angle was defined as the angle between the crystal long axis [210] of TIPS pentacene and a baseline direction [88]. Besides TIPS pentacene, crystal misorientation angle has also been reported in two other organic semiconductors, i.e., 5,6,11,12-tetrachlorotetracene and SMDPPEH. The organic semiconductor 5,6,11,12-tetrachlorotetracene was deposited on the substrate using simple drop casting, and formed randomly-oriented wires with vertical stacking, leading to a large misorientation angle [76]. By using the same method of simple drop casting, organic semiconductor SMDPPEH formed even more severely misoriented wires. The extent of random orientation and aggregations of SMDPPEH made it impossible to accurately measure the misorientation angle [77]. Previous studies indicated that the mixing of polymeric additives with TIPS pentacene can effectively reduce the misorientation angle of organic semiconductor, thereby reducing the charge carrier



mobility variations and improving the electrical performance consistency from device to device [89].

### 1.3.2 Enlarging grain width

Polymeric additives have been reported to enlarge the grain width of the organic semiconductor crystals [90]. It is well known that the grain boundaries can incorporate crystalline defects and trap centers, which downgrade the charge carrier transport in organic thin film transistors. The correlation between grain width and effective mobility was reported by Chen et al. [29], as indicated in Eq. (2):

$$\frac{1}{\mu_E} = A + \frac{B}{W_G}. \quad (2)$$

In Eq. (2),  $\mu_E$  is the effective hole mobility,  $W_G$  is the grain width of organic semiconductor crystals, and  $A$  and  $B$  are two constants. Thereby, enlarged grain width is correlated with enhanced charge transport because it essentially signifies fewer grain boundaries and reduced defects, and reduces the impact from crystalline defects on charge transport in organic semiconductors.

### 1.3.3 Enhancing electrical stability

Additionally, the incorporation of polymer additives shields the charge transport in the organic semiconductor active layer from the impact from the substrate as well as from the environment, which is due to the hydrophobic nature of the polymeric additive and/or the formation of a polymeric encapsulation layer. For example, in order to protect charge transport in the *N,N'*-1*H*,1*H*-perfluorobutyl dicyanoperylene-carboxydiimide (PDIF-CN<sub>2</sub>) organic semiconductor from the impact of the substrate, both P $\alpha$ MS and PMMA were pre-deposited to passivate the silanol groups on the hydrophilic silicon dioxide before spin coating the organic semiconductor [91]. The hydrophobic nature of P $\alpha$ MS and PMMA repels the absorption of water moistures from the environment and thereby improves the thin film transistor stability over time. On the other hand, the incorporation of the polymer additives into the organic semiconductor induces vertical phase segregation and further forms an encapsulation layer [92–96]. Kim et al. reported that when P $\alpha$ MS was blended with an organic semiconductor diF-TESADT, the spin coating of the blends caused a vertical phase

segregation and formed a top polymeric layer which blocks the oxygen and moistures from the ambient environment [97]. Similarly, the encapsulation effect from vertical phase segregation as a result of blending P $\alpha$ MS was also reported by Kang et al. using TIPS pentacene organic semiconductor [98].

### 1.3.4 Promoting phase segregation

Furthermore, the phase segregation from mixing polymeric additives with organic semiconductors may yield a bilayer or trilayer structure in the active layer, which modulates both crystallization and charge transport [99]. A vertically phase segregated active layer with higher concentration of organic semiconductor at the charge transport interface typically exhibits improved charge transport and higher mobilities [100]. For instance, amorphous polymers including P $\alpha$ MS [101, 102], PMMA [103–106] and PS [107, 108] have been reported to exert a strong effect on facilitating a vertical phase segregation according to previous reports. More interestingly, a series of polyacrylate polymers with different lengths of alkyl side groups can switch the phase segregation between lateral and vertical modes: poly(ethyl acrylate) (PEA), poly(butylacrylate) (PBA), and poly(2-ethylhexyl acrylate) (P2EHA) are three polyacrylate polymers sharing a similar molecular core but comprising two, four and eight carbon atoms in the alkyl side chain [109]. As the side chain grows in its length, a dominant lateral phase segregation for the case of PEA was replaced by a coexistence of both lateral and vertical phase segregation for PBA, and further by a dominant vertical phase segregation for P2EHA. Distinctive thin film morphology and charge transport was observed accordingly dependent on the different phase segregation behaviors.

## 2 P $\alpha$ MS and organic semiconductor mixtures

As described in the previous section, the solution-based growth of small-molecular organic semiconductors have a tendency to yield randomly-aligned crystals, which makes it technically challenging to apply these semiconductor materials for large-scale organic electronic devices that require high performance consistency. Thereby, given these challenges, it is highly desirable to control the bulk crystal

alignment of the organic semiconductors, improve crystalline morphology and enhance charge transport. Here we mainly employ TIPS pentacene as a representative semiconductor material to discuss the various merits of P $\alpha$ MS. In Sects. 2.1 and 2.2, we will review the important reports of utilizing P $\alpha$ MS as additives to align bulk crystal orientations and control the organic semiconductor charge transport. Studies involving TIPS pentacene organic semiconductor are discussed first, followed by reports entailing other organic semiconductors in order to underscore a more general approach. It is important to note that although other polymers such as PMMA, PS, polyethylene glycol (PEG) and tetraethylene glycol (TEG) have also been reported as additives to modulate the organic semiconductor crystallization, P $\alpha$ MS has uniquely demonstrated to reduce the bulk crystal misorientation from solution-based drop casting. Therefore, P $\alpha$ MS is studied as a model polymer additive in this work for its effect on reducing bulk crystal misorientation and modulating charge transport of organic semiconductors. When choosing an additive for a specific organic semiconductor, various factors need to be considered such as the additive solubility and dielectric constant. The additive shall possess decent solubility in the solvent of the organic semiconductor, given that many additives need to be mixed with the organic semiconductor at a 1:1 weight ratio for optimized results. Besides, the dielectric constant of the additive need to be taken into account when determining the total capacitance of the thin film transistor device.

Figure 1a shows the molecular structure of P $\alpha$ MS, while Fig. 1b, c shows the structures of the various solution processed, small-molecular organic semiconductors reviewed in this section, including TIPS pentacene and diF-TESADT. Throughout the discussion of these representative examples, we aim to

demonstrate the significant importance of P $\alpha$ MS in application in organic electronic devices.

## 2.1 P $\alpha$ MS as additives for aligning crystal orientations

Among the various polymeric additives mixed with organic semiconductors, P $\alpha$ MS has been demonstrated to effectively control the semiconductor growth and regulate crystal orientation. He et al. reported the incorporation of the P $\alpha$ MS polymer additive at a 1:1 weight ratio, in order to eliminate the randomness of TIPS pentacene organic crystals [110]. The TIPS pentacene crystals can be depicted by the optical image shown in Fig. 2a: the organic semiconductor adopted a dendritic growth pattern and yielded crystals varying in their long axis or charge transport directions. Besides, the organic TIPS pentacene crystals only covered a section of the substrate. In this case, it became almost impossible to implement these randomly oriented crystals to achieve high-performance large-scale organic electronic applications. As P $\alpha$ MS was incorporated in TIPS pentacene, the resultant thin film was shown in Fig. 2c, d. The crystal randomization has been completely eliminated with the organic crystals aligning towards a uniform direction. Additionally, all substrate areas were covered with the organic semiconductor crystals. By defining the crystal misorientation angle as the angle between the long axis of a TIPS pentacene crystal and that of a baseline crystal, a large misorientation angle of  $43.9^\circ \pm 27.8^\circ$  was reported from the TIPS pentacene organic crystals, whereas a significantly smaller angle of  $2.2^\circ \pm 1^\circ$  was observed with the addition of the P $\alpha$ MS polymer. The organic thin film transistors based on the P $\alpha$ MS/TIPS pentacene active layer yielded an enhanced mobility of up to  $0.26 \text{ cm}^2/\text{V s}$ . The performance consistency of the thin film transistors (device schematic is shown

**Fig. 1** Molecular structures of **a** P $\alpha$ MS as well as various organic semiconductors reviewed in this work including **b** TIPS pentacene and **c** diF-TESADT

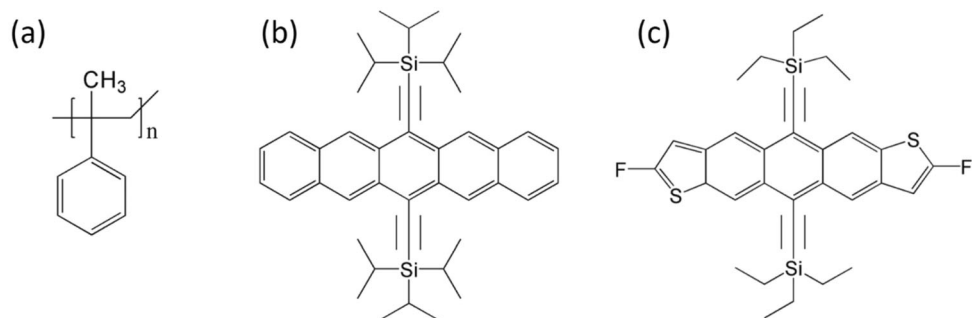
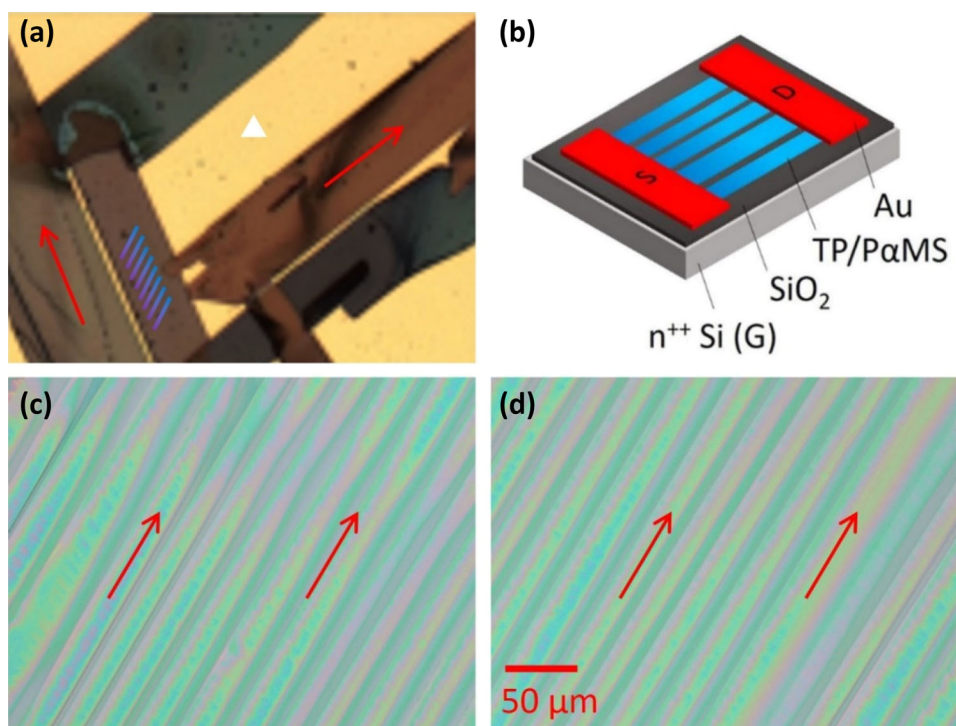


**Fig. 2** Optical photos of **a** TIPS pentacene and **c**, **d** TIPS pentacene/P $\alpha$ MS crystals. **b** Schematic of a bottom-gate, top-contact transistor with gold (Au) as the source (S) and drain (D) electrodes, TIPS pentacene/P $\alpha$ MS as the active layer, and SiO<sub>2</sub> as the gate insulator. Reproduced from [110] with permission from Springer



in Fig. 2b) was denoted by the ratio of the average mobility to the mobility standard deviation. The pristine TIPS pentacene organic crystal thin film transistor was reported to have a performance consistency of 1 [111], indicating the standard deviation of mobility is equivalent to the average mobility. The blend organic crystal based counterpart incorporating P $\alpha$ MS yielded a ratio of up to 3.35, which was a 300% improvement. It can be seen that the addition of the P $\alpha$ MS additive has not only enhanced the mobility but also produced mobilities in a narrower region, indicating improved performance consistency of the TIPS pentacene thin film transistors.

Asaree-Yeboah et al. combined the incorporation of P $\alpha$ MS polymer additive ( $M_w$  108 K) with a temperature gradient technique to eliminate the problem of thermal cracks and to improve film uniformity of TIPS pentacene organic crystals [112]. The temperature gradient technique applied heating to the substrate and allowed the substrate temperature to gradually increase from one side to the other, resulting in different concentrations of solutes across the substrate. In particular, the solution exposed to a lower temperature hosts more solutes and reaches supersaturation sooner than the counterpart exposed to a higher temperature. Then, nucleation sites were formed at the lower temperature side, from which

TIPS pentacene started to crystallize and grow towards the higher temperature side, as illustrated by the schematic of Fig. 3g. The resultant morphology of organic TIPS pentacene crystals was shown in Fig. 3a–c, which implied that the crystals were formed along a fairly uniform direction in spite of the thermal cracks. Thereby, P $\alpha$ MS was mixed with the TIPS pentacene organic semiconductor in solution prior to crystal growth. The TIPS pentacene/P $\alpha$ MS mixture morphology was presented in Fig. 3d–f, showing that the P $\alpha$ MS polymer additive, coupled with the temperature gradient technique, not only aligned the crystals but also eliminated the production of thermal cracks. The surface profile of the TIPS pentacene/P $\alpha$ MS mixture crystals grown with the gradient temperature was shown in Fig. 3h, which showed greatly enhanced uniformity in its film topography as compared with that of the pristine TIPS pentacene deposited via a simple drop casting method. Furthermore, the P $\alpha$ MS additive was also implemented along with the temperature gradient technique for fabricating thin film transistors on a flexible ITO/PET substrate. Figure 3i shows a digital picture of the as-fabricated flexible transistor. Hole mobility of up to 0.25 cm<sup>2</sup>/V s and 0.5 cm<sup>2</sup>/V s were obtained based on the silicon substrate/silicon



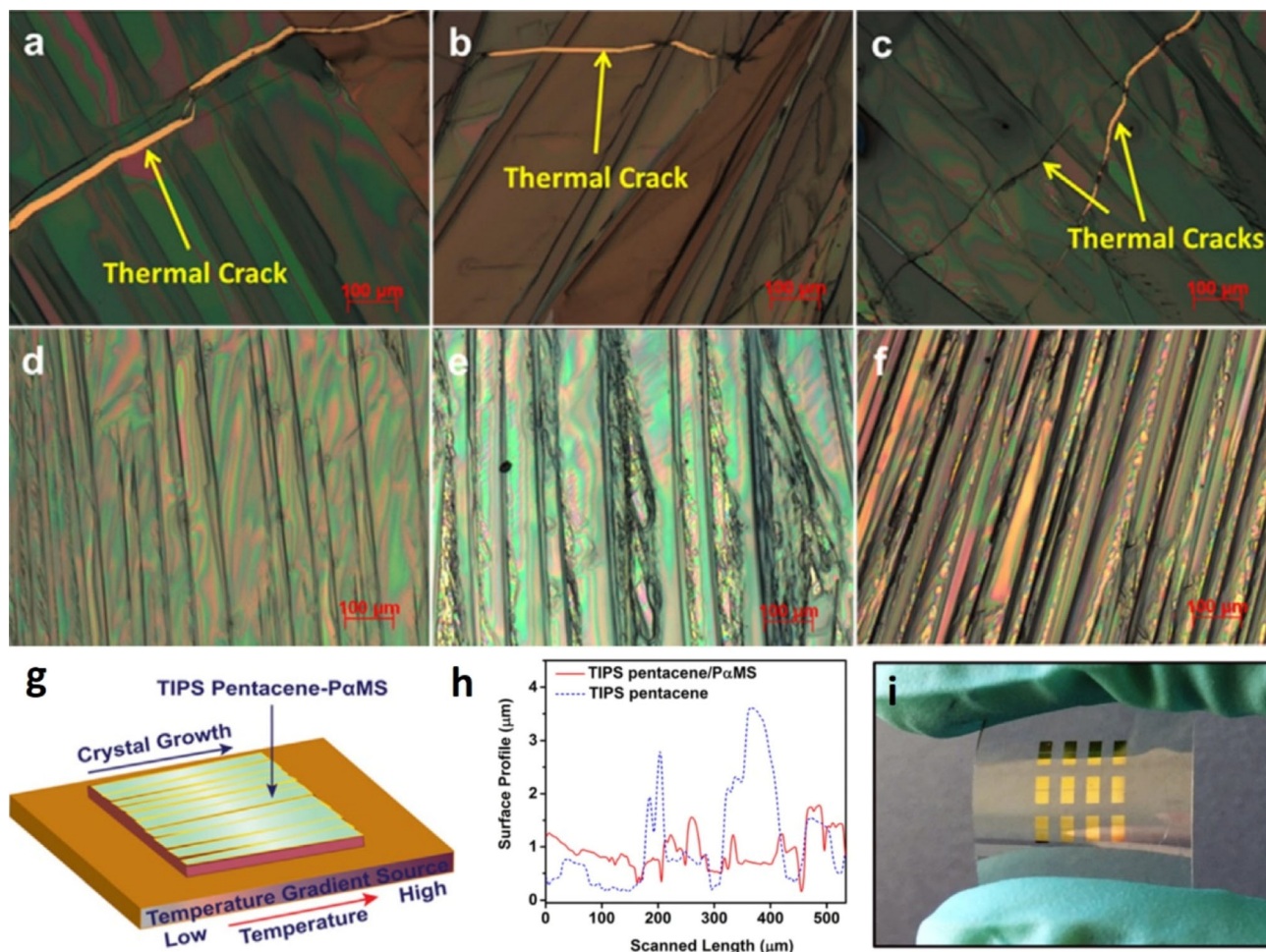


**Fig. 3** Polarized optical images of **a–c** TIPS pentacene films and **d–g** TIPS pentacene/P $\alpha$ MS mixture film, both of which were formed by applying the temperature gradient technique. **g** A schematic showing the mechanism of how the temperature gradient technique aligned the crystal growth of the TIPS

dioxide substrate and flexible ITO/PET substrate, respectively.

Lee et al. reported that the control of 1-dimensional and 2-dimensional crystal growth of TIPS pentacene by mixing with the P $\alpha$ MS ( $M_w$  3160 K) and PMMA ( $M_w$  996 K) as polymer additive [38]. In this work, the function of the P $\alpha$ MS and PMMA polymer additives was mainly to prevent solution dewetting and improve film uniformity, which made it possible to tune the crystal modes between 1 and 2D. By increasing the spin coating time, reduced amount of solvent remained in the mixture which altered the growth mode of TIPS pentacene crystals from 1D mode to 2D mode. In particular, in 1D growth mode, the larger amount of residue solvent resulted in a

pentacene/P $\alpha$ MS mixture. **h** Film topography of both pristine TIPS pentacene from drop casting and aligned TIPS pentacene/P $\alpha$ MS crystals. **i** A digital image showing the as-fabricated flexible thin film transistor device based on the ITO/PET substrate. Reproduced from [112] with permission from Elsevier

shrinking droplet and nucleation at the droplet edge. The convective flow facilitated the crystal to grow from the edge towards the center of the substrate. The 1D growth led to aligned TIPS pentacene crystal ribbons in these localized regions, although crystal misorientation still remained based on the entire substrate. In comparison, when less amount of residue solvent is available in the 2D growth mode, spherulite crystals with large grain size were formed due to random nucleation sites. Besides, vertical phase segregation yielded a bilayer structure with a top TIPS pentacene and a bottom polymer layer. As a result, a higher mobility of  $1.3 \text{ cm}^2/\text{V s}$  was demonstrated from the 2D spherulitic TIPS pentacene crystal based thin film transistors with the P $\alpha$ MS polymer



additive. This work showcases that desired electronic properties of the organic semiconductors can be controlled by tuning the amount of residue solvent.

Sim et al. reported the addition of P $\alpha$ MS into 3,6-bis[5-(4-cyanophenyl)thiophen-2-yl]-2,5-dihexadecylpyrrolo-[3,4-c]pyrrole-1,4(2*H*,5*H*)-dione (DPP-PhCN), which is an n-type cyanophenyl functionalized diketopyrrolopyrrole small-molecule semiconductor, in order to control its crystal growth and orientation [113]. The pristine DPP-PhCN grew into random curved wires with the assistance of cube-induced capillary force. In contrast, the DPP-PhCN/P $\alpha$ MS blends exhibited enhanced alignment in a perpendicular direction towards the tube. In addition to improved alignment, the DPP-PhCN/P $\alpha$ MS microwires showed enlarged length and width. As a result, with the incorporation of the P $\alpha$ MS additive, the DPP-PhCN organic transistors based on cross-linked poly(4-vinylphenol) (CL-PVP) gate dielectric layer demonstrated an enhanced electron mobility of 0.23 cm<sup>2</sup>/V s.

The various works from this section that discussed aligning crystal orientations are summarized in Table 1.

## 2.2 P $\alpha$ MS as additives for modulating semiconductor charge transport

In addition to aligning the orientations of bulk crystals and reducing the crystal misorientations, the incorporation of P $\alpha$ MS polymers has also been demonstrated as a useful pathway to control the morphology and charge transport of the organic

semiconductors. In this section, we will review important works that utilize P $\alpha$ MS polymer as an additive to modify the semiconductor growth and crystallization, enhance the charge carrier mobilities and optimize the performance organic electronic devices.

Hwang et al. reported how P $\alpha$ MS ( $M_w$  100 K) as a polymer additive, in conjunction with solvents with different boiling points, impacted the phase segregation behavior of TIPS pentacene and the compositional structure of the active layer [114]. TIPS pentacene/P $\alpha$ MS mixture was deposited in two different solvents including chlorobenzene and tetralin, which has different boiling point of 132 °C and 207 °C, respectively. The TIPS pentacene/P $\alpha$ MS mixture deposited in chlorobenzene exhibited elongated crystals whereas the same mixture in tetralin showed feather like crystals with much longer crystal length extending in hundreds of micrometers. Accordingly, in the vertical profile, a trilayer structure composed of mainly TIPS pentacene, P $\alpha$ MS and TIPS pentacene was observed from the top to bottom section of the active layer based on the chlorobenzene solvent. In comparison, a bilayer structure comprised of a top TIPS pentacene and bottom P $\alpha$ MS layer was obtained based on the tetralin solvent. The different phase segregation and compositional structures were attributed to the different vapor pressure of the two solvents: a lower vapor pressure allowed more time for TIPS pentacene to phase segregate and crystallize. Thin film transistors with different configurations were fabricated to examine the effect of vertical phase segregation on the semiconductor charge transport. A

**Table 1** A summary of the works reviewed in this section including the authors, various organic semiconductors, molecular weight ( $M_w$ ) of P $\alpha$ MS, the result findings as well as the mobility

Author	Semiconductor	P $\alpha$ MS $M_w$	Result	Mobility
He et al	TIPS pentacene	Not reported	P $\alpha$ MS additive reduced the crystal misorientation and significantly enhanced film morphology uniformity	0.26 cm <sup>2</sup> /V s with the P $\alpha$ MS additive at 1:1 ratio
Asaree-Yeboah et al	TIPS pentacene	108 K	P $\alpha$ MS additive eliminated the thermal cracks caused by temperature gradient technique	0.5 cm <sup>2</sup> /V based on flexible ITO/PET substrate with P $\alpha$ MS additive
Lee et al	TIPS pentacene	3160 K	P $\alpha$ MS additive prevented solution dewetting and improved film uniformity	1.3 cm <sup>2</sup> /V s from 2D spherulitic crystals with P $\alpha$ MS additive
Sim et al	DPP-PhCN	Not reported	P $\alpha$ MS additive attributed to DPP-PhCN alignment in a perpendicular direction towards the tube	0.23 cm <sup>2</sup> /V s with P $\alpha$ MS additive

hole mobility of up to  $0.2 \pm 0.14 \text{ cm}^2/\text{V s}$  was obtained from the top-channel of TIPS pentacene/ $P\alpha\text{MS}$  thin film transistors based on the tetralin solvent.

Ohe et al. studied how the mixing of  $P\alpha\text{MS}$  with TIPS pentacene impacted the phase segregation and vertical compositional structure of the semiconductor [102]. With the secondary ion  $\text{Si}^-$  used as a marker of TIPS pentacene, its three-dimensional distribution observed from time-of-flight secondary ion mass spectrometry (TOF-SIMS) results indicated the semiconductor/polymer mixture is composed of three sublayers. In particular, the top, middle and bottom sublayer is rich of TIPS pentacene,  $P\alpha\text{MS}$  and TIPS pentacene. In order to understand how the morphology and composition changes impact the electrical performance, the ratio of the average standard deviation of on-current to the average on-current was used as a metric for an evaluation. A ratio of 52% and 11% was calculated based on without and with the  $P\alpha\text{MS}$  polymer additive, which implied the polymer additive enhanced the electrical performance consistency of different thin film transistors on the same substrate. Besides, while charge transport in pristine TIPS pentacene thin film transistors was vulnerable to degradation from heat treatment due to the semiconductor structural-phase transition at  $124 \text{ }^\circ\text{C}$ , the  $P\alpha\text{MS}$  polymer additive suppressed such structural degradation and improved thermal stability as the devices were exposed to heating of up to  $180 \text{ }^\circ\text{C}$ . A mobility approximately  $0.12 \text{ cm}^2/\text{V s}$  was reported with the addition of  $P\alpha\text{MS}$ .

Kang et al. performed a study of the effect of  $P\alpha\text{MS}$  polymer additive on the phase segregation and film composition of TIPS pentacene [98], and utilized  $P\alpha\text{MS}$  additive with two different molecular weight including 1.3 K and 575 K. While a trilayered active layer with three different sublayers including a top TIPS pentacene, a middle  $P\alpha\text{MS}$  and then a bottom TIPS pentacene, were observed for  $P\alpha\text{MS}$  with both molecular weight, the  $P\alpha\text{MS}$  with a higher 575 K molecular weight was noticed to yield a bottom layer with a larger thickness of  $117 \text{ \AA}$ . Based on the grazing-incidence X-ray diffraction patterns, the TIPS pentacene film incorporating the high molecular weight  $P\alpha\text{MS}$  showed highly crystalline morphology with an interlayer spacing of  $16.6 \text{ \AA}$ . Besides, the TIPS pentacene molecular layers were desirably oriented parallel to the substrate surface, attributed to improved mobility. As compared with neat TIPS

pentacene thin film transistors with a low average mobility of  $0.05 \text{ cm}^2/\text{V s}$ , the counterpart based on the  $P\alpha\text{MS}$  additive with a higher molecular weight showed an enhanced average mobility of  $0.3 \text{ cm}^2/\text{V s}$ .

Kjellander et al. reported how the different molecular weight of the  $P\alpha\text{MS}$  additive impacted the inkjet printing characteristics and thin film morphology of TIPS pentacene organic semiconductors [115]. In this work, TIPS pentacene was deposited via inkjet printing onto a layer of  $P\alpha\text{MS}$  polymer with different molecular weight of 59 K and 868 K. The inkjet-printed solution droplet was observed to dry out in three different stages. First, a perimeter is formed due to the well-known “coffee ring effect” and contact line pinning. Then, the contact line recedes as the solution droplet shrinks. Finally, a circular center region comprising most crystallized TIPS pentacene is formed as a result of high viscosity as the contact line becomes pinned again. The utilization of the  $P\alpha\text{MS}$  polymer modulated the drying behavior the TIPS pentacene organic semiconductor and led to larger crystalline grains, which was responsible for the improved mobility. Besides,  $P\alpha\text{MS}$  with a higher molecular weight was found to cause the formation of a greater content of TIPS pentacene semiconductor in the perimeter of the inkjet-printed crystalline film. A mobility of up to  $0.7 \text{ cm}^2/\text{V s}$  and  $0.8 \text{ cm}^2/\text{V s}$  were obtained from the TIPS pentacene thin film transistors based on the  $P\alpha\text{MS}$  polymer with the 59 K and 868 K molecular weight, respectively.

Chou et al. utilized the  $P\alpha\text{MS}$  ( $M_w$  100.3 K) for mixing with TIPS pentacene for spray coating applications [116]. While spray coating of pristine TIPS pentacene caused severe dewetting of the organic semiconductor on the substrate, the incorporation of  $P\alpha\text{MS}$  greatly improved the wettability of the film. Different solute concentrations of TIPS pentacene including 10 mg/mL, 15 mg/mL and 20 mg/mL were examined. Highest average mobility was obtained with a concentration of 15 mg/mL, which was attributed to a balance between crystal size across the channel and the crystal grain boundaries. Based on the concentration of 15 mg/mL in the solvent of THN, a loading ratio at 7:3 between TIPS pentacene and  $P\alpha\text{MS}$  yielded continuous crystal needles of TIPS pentacene that cover a large portion of the substrate, giving rise to a hole mobility of up to  $0.323 \text{ cm}^2/\text{V s}$ .

Bae et al. reported the addition of P $\alpha$ MS ( $M_w$  100 K) as a polymer binder for TIPS pentacene based microprinted nonvolatile memory device [117]. In this work, the TIPS pentacene/P $\alpha$ MS mixture was deposited on the substrate and patterned by using a “selective contact evaporation printing” (SCEP) technique. In particular, an elastomeric poly(dimethylsiloxane) (PDMS) mold was brought in contact with the organic semiconductor/polymer solution mixture. As P $\alpha$ MS vertically phase segregated with TIPS pentacene, the mold allowed TIPS pentacene to be absorbed into the PDMS. Subsequently, a thin ferroelectric polymer film, i.e., poly(vinylidene fluoride) (PVDF) and trifluoroethylene (TrFE) copolymers (PVDF–TrFE), was transferred onto the substrate as an insulation layer for the top gate. AFM results indicated that the TIPS pentacene/P $\alpha$ MS blend film exhibited a very uniform surface with a 1.5 nm rms roughness. The TIPS pentacene/P $\alpha$ MS mixture based nonvolatile transistor patterned with the SCEP technique exhibited a mobility of 0.11 cm<sup>2</sup>/V s. The reliability of the memory device was examined by testing the saturation drain current which indicated excellent protection from the ambient environment for up to 10,000 s.

Vaklev et al. reported the employment of a nanolayer of P $\alpha$ MS in order to realize the fabrication of high performance thin film transistors based on two different organic semiconductors including pentacene and TIPS pentacene [118]. In this work, a photolithography patterned PMMA layer was used as the gate dielectric, followed by the deposition of P $\alpha$ MS polymer layer with a thickness of 6 nm. The P $\alpha$ MS layer serves as a non-covalent layer that modifies the surface between the PMMA dielectric layer and the pentacene semiconductor layer, improves the semiconductor packing and enhances its morphology. In addition, the domain size of pentacene crystals deposited based on the P $\alpha$ MS layer was found to be five times larger than the counterpart without P $\alpha$ MS, giving rise to an improved mobility of  $0.6 \pm 0.1$  cm<sup>2</sup>/V s from the pentacene based thin film transistors. On the other hand, the thin film transistors with TIPS pentacene deposited by spin coating and zone casting demonstrated an average mobility of  $0.08 \pm 0.04$  cm<sup>2</sup>/V s and  $0.3 \pm 0.1$  cm<sup>2</sup>/V s based on the P $\alpha$ MS layer, respectively.

Chung et al. reported the addition of P $\alpha$ MS ( $M_w$  420 K) in order to recover the electrical performance

of small molecular semiconductor after exposure to UV radiation, which was described as a “zone-refinement effect” [119]. As the p-type semiconductor triethylsilylethynyl anthradithiophene (TESADT) based thin film transistors were exposed to UV radiation, impurities were introduced in the semiconductor active layer and significantly undermined the charge carrier mobility of TESADT. On the other hand, when P $\alpha$ MS was mixed with TESADT at a mass ratio of 3:7, the polymer additive caused a vertical phase segregation with the organic semiconductor and yielded a TESADT layer free of impurities at the charge transport interface between the gate dielectric layer and semiconductor active layer. While the pristine TESADT thin film transistors exhibited an extremely low mobility around  $10^{-5}$  cm<sup>2</sup>/V s after UV radiation, the counterpart incorporating the P $\alpha$ MS polymer additive showed an enhanced average mobility of up to  $0.040 \pm 0.011$  cm<sup>2</sup>/V s. Similarly, such a zone-refinement effect was also observed in TIPS pentacene organic semiconductor mixed with the P $\alpha$ MS polymer additive. While a low mobility of 0.0083 cm<sup>2</sup>/V s was measured from TIPS pentacene thin film transistors that had been stored in the ambient environment for 3 years, blending P $\alpha$ MS yielded an improved mobility of 0.29 cm<sup>2</sup>/V s, which is comparable to the mobility of freshly-fabricated counterpart.

Niazi et al. reported nucleation and crystallization effect, which is induced by the pentafluorobenzene thiol (PFBT) treatment of gold contact electrodes, on organic semiconductors including diF-TESADT and TIPS pentacene with the P $\alpha$ MS ( $M_w$  100 K) polymer additive [120]. As shown in the optical images of Fig. 4a, the blade coating of TIPS pentacene/P $\alpha$ MS mixture consistently produced ribbon-shaped crystals aligned in the direction of coating, whereas the treatment using PFBT may result in spherulitic crystals on the gold contact electrodes as well as in the charge transport channel when a higher coating speed was applied. Accordingly, the diF-TESADT/P $\alpha$ MS and TIPS pentacene/P $\alpha$ MS mixture based thin film transistors showed a hole mobility of up to 3.6 cm<sup>2</sup>/V s and 4.6 cm<sup>2</sup>/V s without PFBT treatment, respectively, which decreased dramatically for the counterparts with the treatment, as shown in Fig. 4b. In addition, the PFBT treatment on the gold contact electrodes also impacted the vertical phase segregation and compositional structures of the TIPS pentacene/P $\alpha$ MS mixture. As shown in the cross-



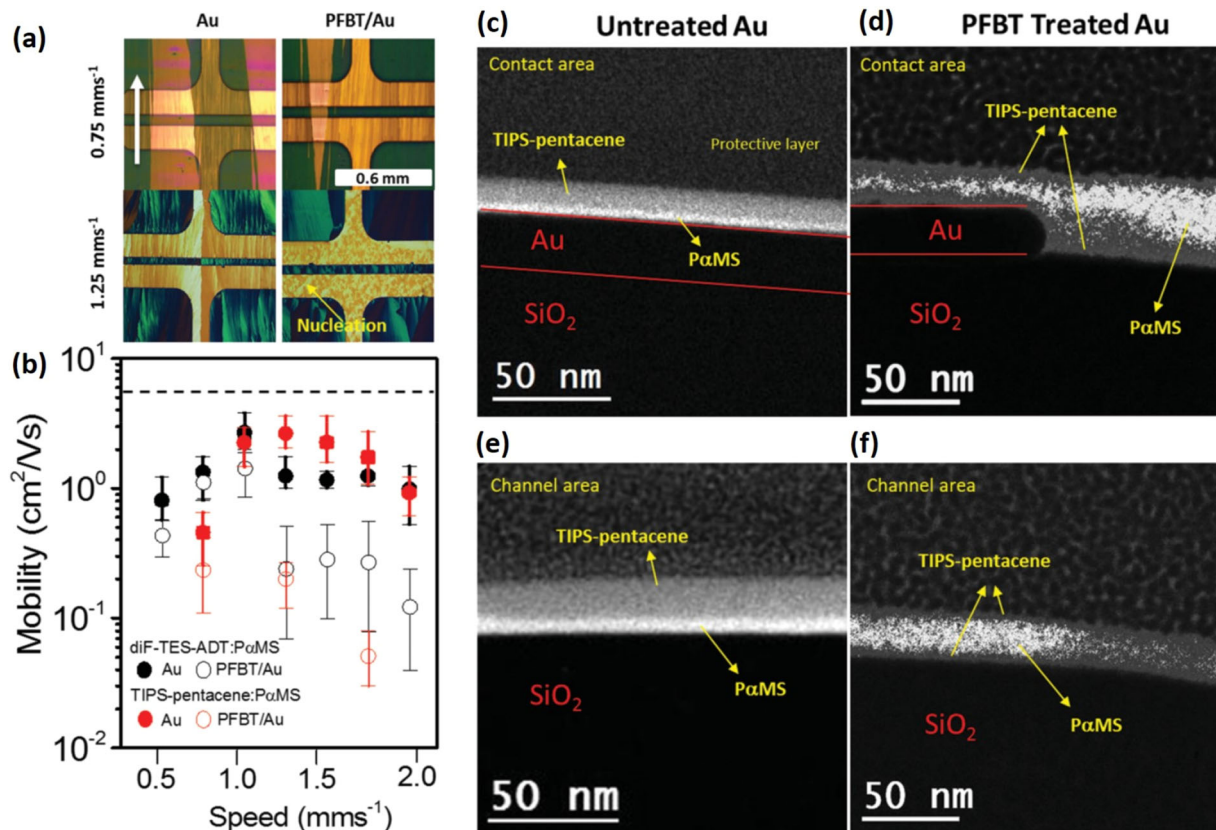


**Fig. 4** **a** Polarized optical microscopic photos showing the morphology of TIPS pentacene/P $\alpha$ MS mixture film on a Si/SiO<sub>2</sub> substrate with and without PFBT treatment on the gold (Au) contact electrodes. Different blade casting speed including 0.75 and 1.25 mm/s were tested. **b** Hole mobility from TIPS pentacene/P $\alpha$ MS blend and diF-TESADT/P $\alpha$ MS blend based thin film

sectional energy-filtered transmission electron microscope (EFTEM) of Fig. 4c, e, the organic semiconductor and polymer additive mixture without the PFBT treatment exhibited a clearly defined vertical phase segregation with a top TIPS pentacene and a bottom P $\alpha$ MS structure within the active layer. In contrast, the PFBT treatment resulted in a different trilayer structure with a top TIPS pentacene, middle P $\alpha$ MS and bottom TIPS pentacene layer, as shown in Fig. 4d, f.

Hamilton et al. reported the addition of P $\alpha$ MS and PTAA polymer additives to improve performance uniformity of two soluble small molecular semiconductors including TIPS pentacene and diF-TESADT [87]. The thin film transistors based on the TIPS pentacene/P $\alpha$ MS blends were fabricated based on two different device configurations including a bottom-contact, top-gate structure and a bottom-contact,

transistors with and without PFBT treatment on Au. c–f Cross-sectional EFTEM images showing the vertical phase separation between TIPS pentacene and P $\alpha$ MS on different substrates with and without PFBT treatment on Au. Reproduced from [120] with permission from Wiley-VCH

dual-gate structure. Higher mobility of 0.69 cm<sup>2</sup>/V s was demonstrated from the transistors with a top gate which was attributed to the higher concentration of vertically phase-segregated TIPS pentacene organic semiconductor in the top channel. In contrast, the organic semiconductors mixed with PTAA yielded a much higher hole mobility of 1.1 cm<sup>2</sup>/V s for TIPS pentacene and 2.41 cm<sup>2</sup>/V s for diF-TESADT, respectively. The improved device performance of PTAA based thin film transistors as compared to the counterparts with P $\alpha$ MS was likely due to the reduced channel width as a result of the lateral phase segregation between the P $\alpha$ MS polymer additive and organic semiconductor. Besides, the use of CYTOP as a dielectric layer for the top gate device was found to improve the operational stability of the thin film transistors. This was because the low permeability of CYTOP to water and oxygen prevents their diffusion

from the ambient environment to the active channel of the transistor device.

He et al. reported the addition of P $\alpha$ MS as a charge trapping layer in order to promote the injection of electrons into the trap states for modulating the charge transport in nonvolatile memory device [121]. In this work, P $\alpha$ MS was deposited via spin coating prior to the thermal evaporation of pentacene as the organic semiconductor active layer. The emission peaks indicated the existence of distribution of defects as recombination centers in the P $\alpha$ MS band-gap. The incorporation of P $\alpha$ MS was estimated to yield energy levels of trap states from 2.9 to 2.51 eV higher than the HOMO of P $\alpha$ MS. By applying a continuous positive gate voltage, the electron injection is promoted along the lateral direction of the channel and results in bulk trap state occupancy. In addition, electrons can be injected along the vertical direction into the trap states of P $\alpha$ MS from the charge transport channel. Consequently, bistable memory behaviors with enlarged memory window is obtained due to the electron transport in the lateral direction from the addition of the P $\alpha$ MS trapping layer.

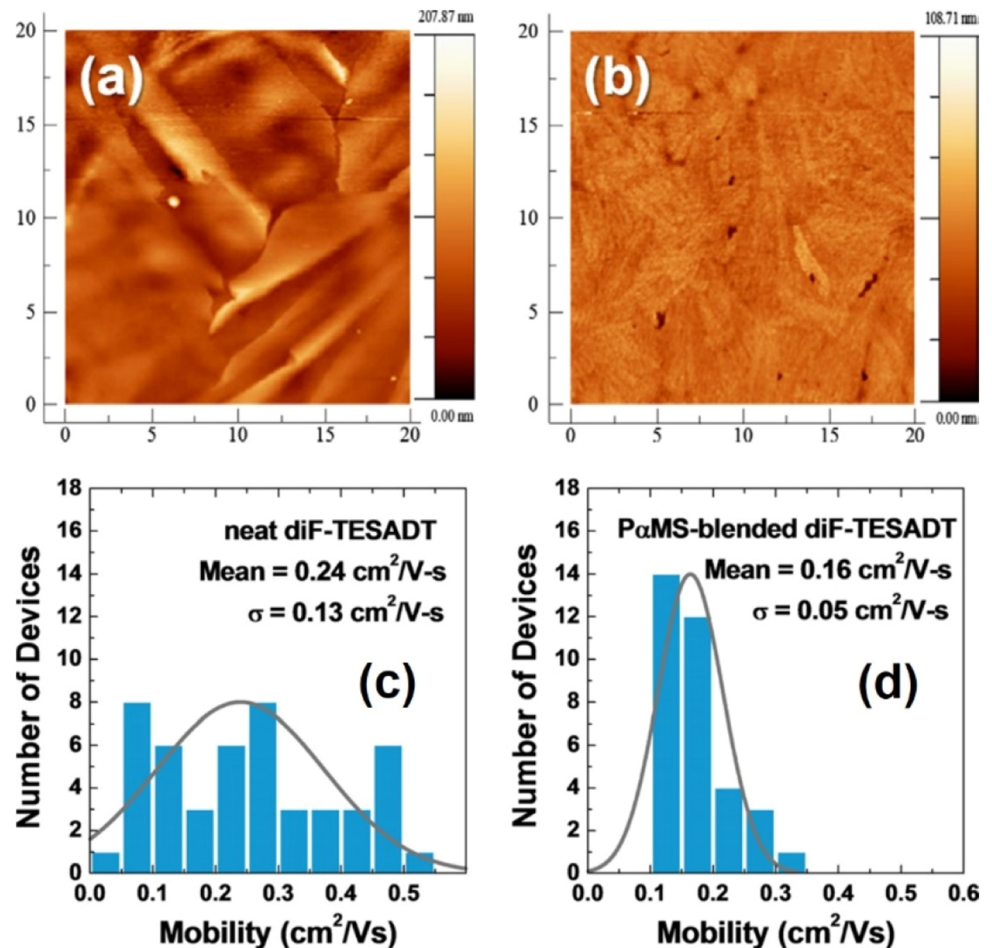
Xu et al. reported a hybrid charge trapping layer comprising HfO<sub>2</sub> and P $\alpha$ MS in order to tune the charge trapping efficiency and device operation speed of the organic nonvolatile memory transistors [122]. In this work, P $\alpha$ MS was spin coated onto the HfO<sub>2</sub> layer, followed by the thermal evaporation of pentacene as the semiconductor layer. Without incorporating the P $\alpha$ MS polymer, the memory device based on the single HfO<sub>2</sub> layer exhibited weak memory effect as a small sweeping voltage was applied. In contrast, the counterpart with the incorporation of P $\alpha$ MS polymer demonstrated a clear memory effect as the sweep voltage increased to 12 V. Such improved performance was attributed to the large grain size of pentacene grown on the hybrid layer of both HfO<sub>2</sub> and P $\alpha$ MS, which gave rise to increased saturation current, more efficient trapping of charges as well as modification effect on the charge transport interface. Besides, the memory device based on the hybrid layer demonstrated a small degradation as going through *P/E* circles, indicating highly reliable operation property.

Kim et al. demonstrated the addition of P $\alpha$ MS into diF-TESADT in order to reduce the mobility variation from device to device and to improve the operational stability [97]. In this work, P $\alpha$ MS ( $M_w$  110 K) was mixed with the organic semiconductor at a 1:1 ratio,

yielding a film morphology with improved uniformity over the whole substrate and in particular in narrow regions between the contact electrodes, as indicated by the AFM images shown in Fig. 5a, b. By testing a total of 30–50 transistor devices, the authors observed a narrower distribution of charge carrier mobility with the incorporation of P $\alpha$ MS as compared to the mobility variation of the pristine diF-TESADT semiconductor, as indicated in the mobility distribution graph in Fig. 5c, d. As a result, an average mobility of  $0.234 \pm 0.13$  cm<sup>2</sup>/V s and  $0.16 \pm 0.05$  cm<sup>2</sup>/V s were demonstrated from the diF-TESADT based thin film transistors without and with P $\alpha$ MS polymer additive, respectively. The much smaller standard deviation of the mobility indicates the enhanced mobility consistency due to the P $\alpha$ MS additive. On the other hand, while oxygen and moistures may diffuse from the ambient environment into the grain boundaries and crystalline structures of the pristine diF-TESADT semiconductor and degrade the device stability of the transistor device, the mixing of the P $\alpha$ MS additive resulted in the formation of an encapsulation layer that effectively prevents the penetration of oxygen and moistures into the active layer, and thereby, enhances the operational stability.

Han et al. reported the incorporation of P $\alpha$ MS ( $M_w$  300 K) as a pre-deposited layer in order to improve the thin film morphology and crystalline structure of inkjet-printed diF-TESADT [123]. Without P $\alpha$ MS, the inkjet printing produced nonuniform semiconductor film with considerable variations in the channel shape. In contrast, the pre-deposition of P $\alpha$ MS polymer layer can be partially dissolved by the ink solution, which gave rise to the formation of a blending zone. As the solution dries, the ink is confined within a fixed dimension and yielded circular-shaped channel with an excellent coverage. In addition, the diF-TESADT/P $\alpha$ MS mixture due to the dissolution of P $\alpha$ MS exhibited a vertical phase segregation with a top diF-TESADT rich layer and a bottom P $\alpha$ MS rich layer. The effect from different solvents including DCB, tetralin and anisole were studied, indicating that the presence of the P $\alpha$ MS layer underneath enlarged the diameter of the organic semiconductor channel. The mobility of neat diF-TESADT was reported to be  $10^{-3}$  cm<sup>2</sup>/V s and  $0.3$  cm<sup>2</sup>/V s based on the solvent of DCB and anisole, respectively. The thin film transistors with the diF-TESADT/P $\alpha$ MS mixture indicated good uniformity in the charge carrier mobilities of  $0.34 \pm 0.13$  cm<sup>2</sup>/V s and

**Fig. 5** AFM images of diF-TESADT films **a** without and **b** with P $\alpha$ MS polymer additive. **c** and **d** Mobility distribution of diF-TESADT thin film transistor without and with P $\alpha$ MS polymer additive. Reproduced from [97] with permission from Elsevier



subthreshold slope of  $0.456 \pm 0.09$  V/decade from the devices.

Shin et al. reported the phase segregation behaviors between diF-TESADT and polymer binders including P $\alpha$ MS ( $M_w$  400 K), PMMA ( $M_w$  190 K) and syndiotactic PS (s-PS) ( $M_w$  250 K) [124]. In particular, P $\alpha$ MS does not contain polar groups, PMMA contains some polar ester groups which would interact with hydrophilic surfaces, and s-PS has its own crystallization events. The resultant diF-TESADT/polymer binder mixture was investigated by using neutron reflectivity and other characterization tools. The diF-TESADT/P $\alpha$ MS mixture exhibited a trilayer structure, comprising a top diF-TESADT layer, a middle P $\alpha$ MS layer and a bottom diF-TESADT layer, which was likely due to the P $\alpha$ MS chains remaining in the middle section of the blend film. The diF-TESADT/PMMA mixture can be divided into a top diF-TESADT layer and a bottom PMMA layer, which was formed as a result of the favorable interaction between the polar PMMA and the hydrophilic polar

silicon dioxide layer. In contrast to the vertical phase segregation for P $\alpha$ MS and PMMA, the diF-TESADT/s-PS mixture was found to exhibit a homogenous structure without stratification. Thin film transistors were fabricated based on the diF-TESADT/polymer binder mixture to test charge transport, yielding a mobility of  $0.094 \pm 0.042$   $\text{cm}^2/\text{V s}$  with P $\alpha$ MS and  $10^{-3}$  to  $10^{-4}$   $\text{cm}^2/\text{V s}$  with both PMMA and s-PS.

Zhong et al. reported the mixing of P $\alpha$ MS ( $M_w$  100 K) with an n-type diketopyrrolopyrrole (DPP) based organic semiconductor, i.e., DPP-CN, to enable the successful device fabrication of thin film transistors [125]. Without the polymer additive, the DPP-CN solution failed to produce a continuous film on the hexamethyldisilazane (HMDS) treated substrate. In contrast, the DPP-CN/P $\alpha$ MS mixture formed continuous spherulitic crystals with extended long-range uniformity. Interestingly, the DPP-CN/P $\alpha$ MS mixture film exhibited two different regions comprised of large and small crystal domains with a surface roughness of 26.2 nm and 47.3 nm, respectively. Due



to a vertically-segregated organic semiconductor top layer, a bottom-contact, top-gate transistor device configuration was used to test charge transport. An electron mobility of up to  $0.5 \text{ cm}^2/\text{V s}$  was measured from the DPP-CN/P $\alpha$ MS mixture based thin film

transistors. Besides, as the thin film transistors were exposed to the ambient environment for 1300 min, the electron mobilities still maintained approximately the same values, implying enhanced air stability of the organic semiconductor DPP-CN.

**Table 2** A summary of the works reviewed in this section including the authors, various organic semiconductors, molecular weight ( $M_w$ ) of P $\alpha$ MS, the result findings as well as the mobility

Author	Semiconductor	P $\alpha$ MS $M_w$	Result	Mobility
Hwang et al	TIPS pentacene	100 K	Different phase segregation and compositional structures were observed due to different solvent vapor pressure	$0.2 \pm 0.14 \text{ cm}^2/\text{V s}$ from the top-channel device with tetralin solvent
Ohe et al	TIPS pentacene	Not reported	Three sublayers with vertical phase segregation were formed due to P $\alpha$ MS additive	$0.12 \text{ cm}^2/\text{V s}$ with P $\alpha$ MS additive
Kang et al	TIPS pentacene	1.3 K and 575 K	A trilayer structure with three sublayers were formed, with sublayer thickness dependent on the molecular weight	$0.3 \text{ cm}^2/\text{V s}$ based on P $\alpha$ MS additive with 575 K $M_w$
Kjellander et al	TIPS pentacene	59 K, 868 K	P $\alpha$ MS with different $M_w$ impacted TIPS pentacene morphology and grain size	$0.8 \text{ cm}^2/\text{V s}$ based on P $\alpha$ MS with a higher $M_w$
Chou et al	TIPS pentacene	100.3 K	P $\alpha$ MS improved the wettability of TIPS pentacene film from spray coating	$0.323 \text{ cm}^2/\text{V s}$ with P $\alpha$ MS additive
Bae et al	TIPS pentacene	100 K	P $\alpha$ MS additive along with a “selective contact evaporation printing” technique was used for fabricating nonvolatile memory device	$0.11 \text{ cm}^2/\text{V s}$ based on TIPS pentacene/P $\alpha$ MS mixture
Vaklev et al	TIPS pentacene, pentacene	Not reported	P $\alpha$ MS as a non-covalent layer modified the charge transport interface, improved semiconductor packing and enhanced its morphology	$0.6 \pm 0.1 \text{ cm}^2/\text{V s}$ and $0.3 \pm 0.1 \text{ cm}^2/\text{V s}$ from pentacene and TIPS pentacene
Chung et al	TIPS pentacene TESADT,	420 K	P $\alpha$ MS caused a vertical phase segregation and a semiconductor layer free of impurities adjacent to charge transport interface	$0.040 \pm 0.011 \text{ cm}^2/\text{V s}$ and $0.29 \text{ cm}^2/\text{V s}$ based on TESADT and TIPS pentacene
Niazi et al	TIPS pentacene, diF-TESADT	100 K	P $\alpha$ MS with PBFT treatment modified phase segregation, morphology and mobility	$3.6 \text{ cm}^2/\text{V s}$ and $4.6 \text{ cm}^2/\text{V s}$ from diF-TESADT and TIPS pentacene with P $\alpha$ MS
Hamilton et al	TIPS pentacene, diF-TESADT	Not reported	P $\alpha$ MS and PTAA were mixed with the semiconductors to improve performance uniformity	$0.69 \text{ cm}^2/\text{V s}$ for TIPS pentacene with P $\alpha$ MS additive
He et al	Pentacene	Not reported	P $\alpha$ MS was used as a charge trapping layer to modify the memory behaviors of memory device	Not reported
Xu et al	Pentacene	Not reported	P $\alpha$ MS was incorporated with HfO <sub>2</sub> as a hybrid charge trapping layer to improve memory device performance	Not reported
Kim et al	diF-TESADT	110 K	P $\alpha$ MS improved the mobility consistency from device to device and formed an encapsulation layer, enhancing operational stability	$0.234 \pm 0.13 \text{ cm}^2/\text{V s}$ and $0.16 \pm 0.05 \text{ cm}^2/\text{V s}$ without and with P $\alpha$ MS
Han et al	diF-TESADT	300 K	P $\alpha$ MS as a pre-deposited layer improved morphology and crystalline structure of inkjet printed diF-TESADT	$0.34 \pm 0.13 \text{ cm}^2/\text{V s}$ with the pre-deposited P $\alpha$ MS layer
Shin et al	diF-TESADT	400 K	P $\alpha$ MS was studied for its phase segregation behavior with diF-TESADT	$0.094 \pm 0.042 \text{ cm}^2/\text{V s}$ with P $\alpha$ MS additive
Zhong et al	DPP-CN	100 K	Continuous spherulitic crystals with extended long-range uniformity were formed due to adding P $\alpha$ MS	$0.5 \text{ cm}^2/\text{V s}$ with P $\alpha$ MS additive

The various works from this section that discussed generally modulating morphology and charge transport are summarized in Table 2.

### 3 Conclusion and future outlook

In this work, we have reviewed P $\alpha$ MS as an important polymeric additive to modulate the crystal orientation and improve charge transport of miscellaneous high-performance solution processable organic semiconductors including TIPS pentacene and diF-TESADT. The significant effect of the P $\alpha$ MS polymer additive on modulating the interfacial surface, improving thin film morphology, mediating phase segregation, enhancing charge transport and reducing mobility variation was discussed based on various organic electronic devices such as organic thin film transistors and memory devices. The influence from different molecular weight of the P $\alpha$ MS polymeric additive on the organic semiconductor was examined, giving rise to different phase segregation behaviors, compositional structures and charge transport. Throughout the discussion of these representative examples, we showcase that P $\alpha$ MS can be implemented to modulate the crystal growth and charge transport of other organic semiconductors beyond the scope of this work.

In addition to P $\alpha$ MS, future works can be dedicated to other types of polymeric additives by studying their effect on controlling the organic semiconductor crystallization and improving the semiconductor crystal orientations. For instance, other insulation polymeric additives such as PMMA and PS can be studied for their capability to improve bulk crystal alignment and reduce crystal misorientation, which shall improve the overall performance consistency of small molecular semiconductor based thin film transistors. Besides, conjugated polymers can effectively modulate the intermolecular interactions between the polymer and organic semiconductors, which offer a new path to tune the charge transport and electrical performance of organic semiconductors [86]. Moreover, semicrystalline polymers combine the properties of both crystalline polymers and amorphous polymers, and thereby, they can improve crystalline film uniformity while simultaneously attributing to charge transport of the organic semiconductors [126]. We believe future studies on these important issues will provide more exciting opportunities to enhance

the charge transport, align crystal growth and expand potential application in organic electronic devices.

### Acknowledgements

S. Bi would like to thank Science and Technology Project of Liaoning Province (20180540006).

### Author contributions

All authors wrote and reviewed this article altogether.

### Data availability

Research data is available upon request.

### Declarations

**Conflict of interest** The authors declare no conflicts of interest.

**Ethical approval** This article does not contain any studies involving animals or human participants performed by any of the authors.

### References

1. K. Amer, A.M. Elshaer, M. Anas, S. Ebrahim, Fabrication, characterization, and electrical measurements of gas ammonia sensor based on organic field effect transistor. *J. Mater. Sci. Mater. Electron.* **30**(1), 391–400 (2019)
2. Z. He, Z. Zhang, S. Bi, Small-molecule additives for organic thin film transistors. *J. Mater. Sci. Mater. Electron.* **30**, 20899–20913 (2019)
3. S. Bi, Q. Li, Y. Yan, K. Asare-Yeboah, T. Ma, C. Tang, Z. Ouyang, Z. He, Y. Liu, C. Jiang, Layer-dependent anisotropic frictional behavior in two-dimensional monolayer hybrid perovskite/ITO layered heterojunctions. *Phys. Chem. Chem. Phys.* **21**(5), 2540–2546 (2019)
4. F. Najafi-Ashtiani, Low temperature processing of BaTiO<sub>3</sub>–PMMA–PVP hybrid films as transparent dielectric gate. *J. Mater. Sci. Mater. Electron.* **30**(7), 7087–7094 (2019)
5. J. Gao, Y. Wang, Y. Han, Y. Gao, C. Wang, L. Han, Y. Zhang, Graphene-based field-effect transistors integrated with microfluidic chip for real-time pH monitoring of seawater. *J. Mater. Sci. Mater. Electron.* **31**(18), 15372–15380 (2020)

6. H. Li, Z. He, Z. Ouyang, S. Palchoudhury, C.W. Ingram, I.I. Harruna, D. Li, Modifying electrical and magnetic properties of single-walled carbon nanotubes by decorating with iron oxide nanoparticles. *J. Nanosci. Nanotechnol.* **20**(4), 2611–2616 (2020)
7. S. Barard, D. Mukherjee, S. Sarkar, T. Kreouzis, I. Chambrier, A.N. Cammidge, A.K. Ray, Channel length-dependent characterisations of organic thin-film transistors with solution processable gadolinium phthalocyanine derivatives. *J. Mater. Sci. Mater. Electron.* **31**(1), 265–273 (2020)
8. K. Bhargava, N. Yadav, N. Kumari, S.S. Pandey, V. Singh, Reduced contact resistance in organic field-effect transistors fabricated using floating film transfer method. *J. Mater. Sci. Mater. Electron.* **31**(18), 15277–15285 (2020)
9. A. Saeed, A. Alshahrie, N. Salah, Fabrication of highly efficient organic light-emitting diode based on dysprosium-incorporated tris-(8-hydroxyquinoline)aluminum. *J. Mater. Sci. Mater. Electron.* (2020). <https://doi.org/10.1007/s10854-020-04721-9>
10. W. Gu, Recent progress on rubrene as active layer in organic field-effect transistors. *J. Nanopart. Res.* **22**(9), 249 (2020)
11. W. Kim, A. Nowak-Król, Y. Hong, F. Schlosser, F. Würthner, D. Kim, Solvent-modulated charge-transfer resonance enhancement in the excimer state of a bay-substituted perylene bisimide cyclophane. *J. Phys. Chem. Lett.* **10**(8), 1919–1927 (2019)
12. M.-W. Kim, S. Kwon, J. Kim, C. Lee, I. Park, J.H. Shim, I.-S. Jeong, Y.-R. Jo, B. Park, J.-H. Lee, K. Lee, B.-J. Kim, Reversible polymorphic transition and hysteresis-driven phase selectivity in single-crystalline C<sub>8</sub>-BTBT rods. *Small* **16**(3), 1906109 (2020)
13. Z. Yang, S. Lin, J. Liu, K. Zheng, G. Lu, B. Ye, J. Huang, Y. Zhang, Y. Ye, T. Guo, G. Chen, Integration of highly crystalline C<sub>8</sub>-BTBT thin-films into simple logic gates and circuits. *Org. Electron.* **78**, 64–71 (2020)
14. T. Shen, H. Zhou, X. Liu, Y. Fan, D.D. Mishra, Q. Fan, Z. Yang, X. Wang, M. Zhang, J. Li, Wettability control of interfaces for high-performance organic thin-film transistors by soluble insulating polymer films. *ACS Omega* **5**(19), 10891–10899 (2020)
15. N. Onojima, N. Akiyama, Y. Mori, T. Sugai, S. Obata, Small molecule/polymer blends prepared by environmentally-friendly process for mechanically-stable flexible organic field-effect transistors. *Org. Electron.* **78**, 105597 (2020)
16. X. Xiao, G. Pan, F. Zhang, High transparency and enhanced mobility of field-effect transistors of the semiconductor/insulator polymer blends with ultralow semiconductor content. *Org. Electron.* **82**, 105709 (2020)
17. Z. Yang, S. Lin, J. Liu, K. Zheng, G. Lu, B. Ye, J. Huang, Y. Zhang, Y. Ye, T. Guo, G. Chen, Efficient combination of Roll-to-Roll compatible techniques towards the large area deposition of a polymer dielectric film and the solution-processing of an organic semiconductor for the field-effect transistors fabrication on plastic substrate. *Org. Electron.* **78**, 231–239 (2020)
18. S. Bi, W. Zhao, Y. Sun, C. Jiang, Y. Liu, Z. He, Q. Li, J. Song, Dynamic photonic perovskite light-emitting diodes with post-treatment-enhanced crystallization as writable and wipeable inscribers. *Nanoscale Adv.* **3**(23), 6659–6668 (2021)
19. R.J. Hudson, J.M. de la Perrelle, R.D. Pensack, B. Kudisch, G.D. Scholes, D.M. Huang, T.W. Kee, Organizing crystalline functionalized pentacene using periodicity of poly(vinyl alcohol). *J. Phys. Chem. Lett.* **11**(2), 516–523 (2020)
20. Z.R. Wang, Y. Zou, W.Q. Chen, Y.J. Huang, C.J. Yao, Q.C. Zhang, The role of weak molecular dopants in enhancing the performance of solution-processed organic field-effect transistors. *Adv. Electron. Mater.* **5**(2), 1800547 (2019)
21. Z. He, J. Chen, J.K. Keum, G. Szulczewski, D. Li, Improving performance of TIPS pentacene-based organic thin film transistors with small-molecule additives. *Org. Electron.* **15**(1), 150–155 (2014)
22. X.M. Zhuang, S.J. Han, B.X. Huai, W. Shi, J.S. Yu, Sub-ppm and high response organic thin-film transistor NO<sub>2</sub> sensor based on nanofibrillar structured TIPS-pentacene. *Sens. Actuators B* **279**, 238–244 (2019)
23. B. Shao, Y. Liu, X. Zhuang, S. Hou, S. Han, X. Yu, J. Yu, Crystallinity and grain boundary control of TIPS-pentacene in organic thin-film transistors for the ultra-high sensitive detection of NO<sub>2</sub>. *J. Mater. Chem. C* **7**(33), 10196–10202 (2019)
24. Y. Sun, Z. Zhang, K. Asare-Yeboah, S. Bi, Z. He, Poly(-butyl acrylate) polymer enhanced phase segregation and morphology of organic semiconductor for solution-processed thin film transistors. *J. Appl. Polym. Sci.* **138**(27), 50654 (2021)
25. J.S. Brooks, D.L. Eaton, J.E. Anthony, S.R. Parkin, J.W. Brill, Y. Sushko, Electronic and optical properties of functionalized pentacene compounds in the solid state. *Org. Electron.* **1**(4), 301–306 (2001)
26. C.D. Sheraw, T.N. Jackson, D.L. Eaton, J.E. Anthony, Functionalized pentacene active layer organic thin-film transistors. *Adv. Mater.* **15**(23), 2009–2011 (2003)
27. J.H. Chen, D.C. Martin, J.E. Anthony, Morphology and molecular orientation of thin-film



- bis(triisopropylsilylethynyl) pentacene. *J. Mater. Res.* **22**(6), 1701–1709 (2007)
28. Z. He, Z. Zhang, S. Bi, Long-range crystal alignment with polymer additive for organic thin film transistors. *J. Polym. Res.* **26**(7), 173 (2019)
29. J.H. Chen, C.K. Tee, M. Shtein, J. Anthony, D.C. Martin, Grain-boundary-limited charge transport in solution-processed 6,13 bis(tri-isopropylsilylethynyl) pentacene thin film transistors. *J. Appl. Phys.* **103**(11), 114513 (2008)
30. Z. He, Z. Zhang, S. Bi, Nanoscale alignment of semiconductor crystals for high-fidelity organic electronics applications. *Appl. Nanosci.* **11**, 787–795 (2019)
31. J.H. Chen, C.K. Tee, J.Y. Yang, C. Shaw, M. Shtein, J. Anthony, D.C. Martin, Thermal and mechanical cracking in bis(triisopropylsilylethynyl) pentacene thin films. *J. Polym. Sci. B* **44**(24), 3631–3641 (2006)
32. Z. He, K. Asare-Yeboah, Z. Zhang, S. Bi, Self-assembly crystal microribbons with nucleation additive for high-performance organic thin film transistors. *Jpn. J. Appl. Phys.* **58**, 061009 (2019)
33. D.H. Kim, D.Y. Lee, H.S. Lee, W.H. Lee, Y.H. Kim, J.I. Han, K. Cho, High-mobility organic transistors based on single-crystalline microribbons of triisopropylsilylethynyl pentacene via solution-phase self-assembly. *Adv. Mater.* **19**(5), 678–682 (2007)
34. J.H. Chen, J.E. Anthony, D.C. Martin, Crystallographic cracking during a thermally-induced solid-state phase transition in TIPS pentacene. *Abstr. Pap. Am. Chem. Soc.* **230**, 309-POLY (2005)
35. J.H. Chen, S. Subramanian, S.R. Parkin, M. Siegler, K. Gallup, C. Haughn, D.C. Martin, J.E. Anthony, The influence of side chains on the structures and properties of functionalized pentacenes. *J. Mater. Chem.* **18**(17), 1961–1969 (2008)
36. Z. He, Z. Zhang, S. Bi, K. Asare-Yeboah, J. Chen, Ultra-low misorientation angle in small-molecule semiconductor/polyethylene oxide blends for organic thin film transistors. *J. Polym. Res.* **27**(3), 75 (2020)
37. Z. He, Z. Zhang, S. Bi, K. Asare-Yeboah, J. Chen, D. Li, A facile and novel route to improve TIPS pentacene based organic thin film transistor performance with elastomer. *Synth. Met.* **262**, 116337 (2020)
38. J.H. Lee, H.H. Choi, Y.D. Park, J.E. Anthony, J.A. Lim, J. Cho, D.S. Chung, J. Hwang, H.W. Jang, K. Cho, W.H. Lee, 1D versus 2D growth of soluble acene crystals from soluble acene/polymer blends governed by a residual solvent reservoir in a phase-separated polymer matrix. *Adv. Funct. Mater.* **28**(34), 1802875 (2018)
39. K. Kim, K. Nam, X. Li, D.Y. Lee, S.H. Kim, Programmed design of highly crystalline organic semiconductor patterns with uniaxial alignment via blade coating for high-performance organic field-effect. *ACS Appl. Mater. Interfaces* **11**(45), 42403–42411 (2019)
40. S. Wang, S. Zhou, Y. Tong, Z. Song, H. Wang, Q. Tang, X. Zhao, Y. Liu, Dielectric selection for solution-processed high-mobility TIPS-pentacene microwire field-effect transistors. *Adv. Mater. Interfaces* **6**(13), 1801984 (2019)
41. D. Bharti, S.P. Tiwari, Phase separation induced high mobility and electrical stability in organic field-effect transistors. *Synth. Met.* **221**, 186–191 (2016)
42. C.T. da Rocha, K. Haase, Y.C. Zheng, M. Löffler, M. Hamsch, S.C.B. Mannsfeld, Solution coating of small molecule/polymer blends enabling ultralow voltage and high-mobility organic transistors. *Adv. Electron. Mater.* **4**(8), 1800141 (2018)
43. Y. Diao, B.C.K. Tee, G. Giri, J. Xu, D.H. Kim, H.A. Becerril, R.M. Stoltenberg, T.H. Lee, G. Xue, S.C.B. Mannsfeld, Z.N. Bao, Solution coating of large-area organic semiconductor thin films with aligned single-crystalline domains. *Nat. Mater.* **12**(7), 665–671 (2013)
44. Y.J. Su, X. Gao, J.G. Liu, R.B. Xing, Y.C. Han, Uniaxial alignment of triisopropylsilylethynyl pentacene via zone-casting technique. *Phys. Chem. Chem. Phys.* **15**(34), 14396–14404 (2013)
45. D.H. Kim, J.A. Lim, W. Cha, J.H. Lee, H. Kim, J.H. Cho, Directed self-assembly of organic semiconductors via confined evaporative capillary flows for use in organic field-effect transistors. *Org. Electron.* **15**(10), 2322–2327 (2014)
46. T. Shen, H. Zhou, J. Xin, Q. Fan, Z. Yang, J. Wang, T. Mei, X. Wang, N. Wang, J. Li, Controllable microstructure of polymer-small molecule blend thin films for high-performance organic field-effect transistors. *Appl. Surf. Sci.* **498**, 143822 (2019)
47. K. Haase, C.T. da Rocha, C. Hauenstein, Y.C. Zheng, M. Hamsch, S.C.B. Mannsfeld, High-mobility, solution-processed organic field-effect transistors from C<sub>8</sub>-BTBT:polystyrene blends. *Adv. Electron. Mater.* **4**(8), 1800076 (2018)
48. J. Panidi, A.F. Paterson, D. Khim, Z.P. Fei, Y. Han, L. Tsetseris, G. Vourlias, P.A. Patsalas, M. Heeney, T.D. Anthopoulos, Remarkable enhancement of the hole mobility in several organic small-molecules, polymers, and small-molecule:polymer blend transistors by simple admixing of the Lewis acid p-dopant B(C<sub>6</sub>F<sub>5</sub>)<sub>3</sub>. *Adv. Sci.* **5**(1), 1700290 (2018)
49. X. Zhang, W. Deng, B. Lu, X. Fang, X. Zhang, J. Jie, Fast deposition of an ultrathin, highly crystalline organic semiconductor film for high-performance transistors. *Nanoscale Horiz.* **5**(7), 1096–1105 (2020)

50. Z. He, Z. Zhang, S. Bi, J. Chen, Effect of polymer molecular weight on morphology and charge transport of small-molecular organic semiconductors. *Electron. Mater. Lett.* **16**(5), 441–450 (2020)
51. Z. He, Z. Zhang, S. Bi, J. Chen, D. Li, Conjugated polymer controlled morphology and charge transport of small-molecule organic semiconductors. *Sci. Rep.* **10**(1), 4344 (2020)
52. H.D. Fan, S.J. Han, Z.H. Song, J.S. Yu, H.E. Katz, Organic field-effect transistor gas sensor based on GO/PMMA hybrid dielectric for the enhancement of sensitivity and selectivity to ammonia. *Org. Electron.* **67**, 247–252 (2019)
53. X. Zhuang, S. Han, B. Huai, W. Shi, Y. Junsheng, Sub-ppm and high response organic thin-film transistor NO<sub>2</sub> sensor based on nanofibrillar structured TIPS-pentacene. *Sens. Actuators B* **279**(14), 238–244 (2019)
54. K. Asare-Yeboah, Q. Li, C. Jiang, Z. He, S. Bi, Y. Liu, C. Liu, High performance and efficiency resonant photo-effect-transistor by near-field nano-strip-controlled organic light emitting diode gate. *J. Phys. Chem. Lett.* **11**(16), 6526–6534 (2020)
55. Q. Li, C. Jiang, S. Bi, K. Asare-Yeboah, Z. He, Y. Liu, Photo-triggered logic circuits assembled on integrated illuminants and resonant nanowires. *ACS Appl. Mater. Interfaces* **12**(24), 46501–46508 (2020)
56. S. Bi, Q. Li, Z. He, Q. Guo, K. Asare-Yeboah, Y. Liu, C. Jiang, Highly enhanced performance of integrated piezo photo-transistor with dual inverted OLED gate and nanowire array channel. *Nano Energy* **66**, 104101 (2019)
57. C.M. Benavides, M. Biele, O. Schmidt, C.J. Brabec, S.F. Tedde, TIPS pentacene as a beneficial interlayer for organic photodetectors in imaging applications. *IEEE Trans. Electron Devices* **65**(4), 1516–1522 (2018)
58. J.H. Kwon, S.I. Shin, C.H. Kim, I.K. You, C.I. Cho, B.K. Ju, Flexible organic thin-film transistors for photodetectors. *J. Korean Phys. Soc.* **55**(1), 72–75 (2009)
59. H. Yamauchi, M. Sakai, S. Kuniyoshi, K. Kudo, Fabrication of n- and p-channel step-edge vertical-channel transistors by electro spray deposition. *Jpn. J. Appl. Phys.* **53**(1), 01AB16 (2014)
60. S. Park, B. Lee, B. Bae, J. Chai, S. Lee, C. Kim, Ambipolar thin-film transistors based on organic semiconductor blend. *Synth. Met.* **253**, 40–47 (2019)
61. S. Hou, J. Yu, X. Zhuang, D. Li, Y. Liu, Z. Gao, T. Sun, F. Wang, X. Yu, Phase separation of P3HT/PMMA blend film formed semiconducting and dielectric layers in organic thin film transistors for high sensitivity NO<sub>2</sub> detection. *ACS Appl. Electron. Mater.* **11**(47), 44521–44527 (2019)
62. H. Yang, H.-C. Kwon, S. Ma, K. Kim, S.-C. Yun, G. Jang, J. Park, H. Lee, S. Goh, J. Moon, Energy-level graded Al-doped ZnO protection layer for copper nanowire-based window electrodes for efficient flexible perovskite solar cells. *ACS Appl. Mater. Interfaces* **12**(12), 13824–13835 (2020)
63. H.Y. Li, B.C.K. Tee, G. Giri, J.W. Chung, S.Y. Lee, Z.N. Bao, High-performance transistors and complementary inverters based on solution-grown aligned organic single-crystals. *Adv. Mater.* **24**(19), 2588–2591 (2012)
64. J. Li, Y. Zhao, H.S. Tan, Y.L. Guo, C.A. Di, G. Yu, Y.Q. Liu, M. Lin, S.H. Lim, Y.H. Zhou, H.B. Su, B.S. Ong, A stable solution-processed polymer semiconductor with record high-mobility for printed transistors. *Sci. Rep.* **2**, 754 (2012)
65. J.B. Kim, C. Fuentes-Hernandez, D.K. Hwang, S.P. Tiwari, W.J. Potscavage, B. Kippelen, Vertically stacked complementary inverters with solution-processed organic semiconductors. *Org. Electron.* **12**(7), 1132–1136 (2011)
66. R. Colucci, H.F. de Paula Barbosa, F. Günther, P. Cavassin, G.C. Faria, Recent advances in modeling organic electrochemical transistors. *Flex. Print. Electron.* **5**(1), 013001 (2020)
67. Q. Li, Y. Guo, Y. Liu, Exploration of near-infrared organic photodetectors. *Chem. Mater.* **31**(17), 6359–6379 (2019)
68. B. Wood, K.P. Girard, C.S. Polster, D.M. Croker, Progress to date in the design and operation of continuous crystallization processes for pharmaceutical applications. *Org. Process Res. Dev.* **23**(2), 122–144 (2019)
69. J.H. Kwon, J.H. Seo, S.I. Shin, K.H. Kim, D.H. Choi, I.B. Kang, H. Kang, B.K. Ju, A 6,13-bis(triisopropylsilyl)ethynyl pentacene thin-film transistor using a spun-on inorganic gate-dielectric. *IEEE Trans. Electron Devices* **55**(2), 500–505 (2008)
70. S.H. Lee, M.H. Choi, S.H. Han, D.J. Choo, J. Jang, S.K. Kwon, High-performance thin-film transistor with 6,13-bis(triisopropylsilyl)ethynyl pentacene by inkjet printing. *Org. Electron.* **9**(5), 721–726 (2008)
71. Z. He, K. Xiao, W. Durant, D.K. Hensley, J.E. Anthony, K. Hong, S.M. Kilbey II, J. Chen, D. Li, Enhanced performance consistency in nanoparticle/TIPS pentacene-based organic thin film transistors. *Adv. Funct. Mater.* **21**(19), 3617–3623 (2011)
72. Z. He, J. Chen, D. Li, Crystal alignment for high performance organic electronics devices. *J. Vac. Sci. Technol. A* **37**(4), 040801 (2019)
73. L. Zhang, N. Pastukova, Y.F. Yao, X.L. Zhong, E. Pavlica, G. Bratina, E. Orgiu, P. Samori, Self-suspended nanomesh scaffold for ultrafast flexible photodetectors based on organic semiconducting crystals. *Adv. Mater.* **30**(28), 1801181 (2018)

74. J.H. Chen, C.K. Tee, M. Shtein, D.C. Martin, J. Anthony, Controlled solution deposition and systematic study of charge-transport anisotropy in single crystal and single-crystal textured TIPS pentacene thin films. *Org. Electron.* **10**(4), 696–703 (2009)
75. H.B. Akkerman, H.Y. Li, Z.N. Bao, TIPS-pentacene crystalline thin film growth. *Org. Electron.* **13**(10), 2056–2062 (2012)
76. Z. He, N. Lopez, X. Chi, D. Li, Solution-based 5,6,11,12-tetrachlorotetracene crystal growth for high-performance organic thin film transistors. *Org. Electron.* **22**, 191–196 (2015)
77. S. Bi, Z. He, J. Chen, D. Li, Solution-grown small-molecule organic semiconductor with enhanced crystal alignment and areal coverage for organic thin film transistors. *AIP Adv.* **5**(7), 077170 (2015)
78. S. Bi, Y. Li, Z. He, Z. Ouyang, Q. Guo, C. Jiang, Self-assembly diketopyrrolopyrrole-based materials and polymer blend with enhanced crystal alignment and property for organic field-effect transistors. *Org. Electron.* **65**, 96–99 (2019)
79. D.T. James, J.M. Frost, J. Wade, J. Nelson, J.S. Kim, Controlling microstructure of pentacene derivatives by solution processing: impact of structural anisotropy on optoelectronic properties. *ACS Nano* **7**(9), 7983–7991 (2013)
80. Y. Li, C. Liu, A. Kumatani, P. Darmawan, T. Minari, K. Tsukagoshi, Large plate-like organic crystals from direct spin-coating for solution-processed field-effect transistor arrays with high uniformity. *Org. Electron.* **13**(2), 264–272 (2012)
81. K. Asare-Yeboah, R.M. Frazier, G. Szulczewski, D. Li, Temperature gradient approach to grow large, preferentially oriented 6,13-bis(triisopropylsilylethynyl) pentacene crystals for organic thin film transistors. *J. Vac. Sci. Technol. B* **32**(5), 052401 (2014)
82. G.W. Kim, M. Kim, Y.D. Park, Effect of solvent exchange at the biphasic dip-coating interface on the formation of polythiophene thin films. *J. Phys. Chem. C* **122**(4), 2432–2439 (2018)
83. H. Opoku, B. Nketia-Yawson, E.-S. Shin, Y.-Y. Noh, Organic field-effect transistors processed by an environmentally friendly non-halogenated solvent blend. *J. Mater. Chem. C* **6**(3), 661–667 (2018)
84. Z. He, Z. Zhang, K. Asare-Yeboah, S. Bi, J. Chen, D. Li, Crystal growth of small-molecule organic semiconductors with nucleation additive. *Curr. Appl. Phys.* **21**, 107–115 (2021)
85. D.T. James, B.K.C. Kjellander, W.T.T. Smaal, G.H. Gelinck, C. Combe, I. McCulloch, R. Wilson, J.H. Burroughes, D.D.C. Bradley, J.S. Kim, Thin-film morphology of inkjet-printed single-droplet organic transistors using polarized Raman spectroscopy: effect of blending TIPS-pentacene with insulating polymer. *ACS Nano* **5**(12), 9824–9835 (2011)
86. J. Chen, M. Shao, K. Xiao, Z. He, D. Li, B.S. Lokitz, D.K. Hensley, S.M. Kilbey II., J.E. Anthony, J.K. Keum, A.J. Rondinone, W.-Y. Lee, S. Hong, Z. Bao, Conjugated polymer-mediated polymorphism of a high performance, small-molecule organic semiconductor with tuned intermolecular interactions, enhanced long-range order, and charge transport. *Chem. Mater.* **25**(21), 4378–4386 (2013)
87. R. Hamilton, J. Smith, S. Ogier, M. Heeney, J.E. Anthony, I. McCulloch, J. Veres, D.D.C. Bradley, T.D. Anthopoulos, High-performance polymer–small molecule blend organic transistors. *Adv. Mater.* **21**(10–11), 1166–1171 (2009)
88. Z. He, Z. Zhang, S. Bi, Nanoparticles for organic electronics applications. *Mater. Res. Express* **7**, 012004 (2020)
89. W. Sun, J. Zhao, S. Chen, X. Guo, Q. Zhang, Thermally cross-linked polyvinyl alcohol as gate dielectrics for solution processing organic field-effect transistors. *Synth. Met.* **250**, 73–78 (2019)
90. Y. Sun, Z. Zhang, K. Asare-Yeboah, S. Bi, Z. He, Large-dimensional organic semiconductor crystals with poly(butyl acrylate) polymer for solution-processed organic thin film transistors. *Electron. Mater. Lett.* **17**, 33–42 (2021)
91. Z. He, S. Shaik, S. Bi, J. Chen, D. Li, Air-stable solution-processed n-channel organic thin film transistors with polymer-enhanced morphology. *Appl. Phys. Lett.* **106**(18), 183301 (2015)
92. N. Onojima, K. Hara, A. Nakamura, Vertical phase separation of 6,13-bis(triisopropylsilylethynyl) pentacene/poly(methyl methacrylate) blends prepared by electrostatic spray deposition for organic field-effect transistors. *Jpn. J. Appl. Phys.* **56**, 5S2 (2017)
93. Z. He, Z. Zhang, S. Bi, Polyacrylate polymer assisted crystallization: improved charge transport and performance consistency for solution-processable small-molecule semiconductor based organic thin film transistors. *J. Sci. Adv. Mater. Devices* **4**(3), 467–472 (2019)
94. K. Zhao, O. Wodo, D. Ren, H.U. Khan, M.R. Niazi, H. Hu, M. Abdelsamie, R. Li, E.Q. Li, L. Yu, B. Yan, M.M. Payne, J. Smith, J.E. Anthony, T.D. Anthopoulos, S.T. Thoroddsen, B. Ganapathysubramanian, A. Amassian, Vertical phase separation in small molecule polymer blend organic thin film transistors can be dynamically controlled. *Adv. Funct. Mater.* **26**(11), 1737–1746 (2016)
95. X. Lei, S. Ge, Y. Tan, Z. Wang, J. Li, X. Li, G. Hu, X. Zhu, M. Huang, Y. Zhu, B. Xiang, High capacity and energy density of Zn–Ni–Co–P nanowire arrays as an advanced

- electrode for aqueous asymmetric supercapacitor. *ACS Appl. Mater. Interfaces* **12**(8), 9158–9168 (2020)
96. J. Smith, R. Hamilton, I. McCulloch, N. Stingelin-Stutzmann, M. Heeney, D.D.C. Bradley, T.D. Anthopoulos, Solution-processed organic transistors based on semiconducting blends. *J. Mater. Chem.* **20**(13), 2562–2574 (2010)
97. Y.H. Kim, J.E. Anthony, S.K. Park, Polymer blended small molecule organic field effect transistors with improved device-to-device uniformity and operational stability. *Org. Electron.* **13**(7), 1152–1157 (2012)
98. J. Kang, N. Shin, D.Y. Jang, V.M. Prabhu, D.Y. Yoon, Structure and properties of small molecule–polymer blend semiconductors for organic thin film transistors. *J. Am. Chem. Soc.* **130**(37), 12273–12275 (2008)
99. Z. Zhang, Z. He, S. Bi, K. Asare-Yeboah, Phase segregation controlled semiconductor crystallization for organic thin film transistors. *J. Sci. Adv. Mater. Devices* **5**(2), 151–163 (2020)
100. Z. He, S. Bi, K. Asare-Yeboah, Z. Zhang, Phase segregation effect on TIPS pentacene crystallization and morphology for organic thin film transistors. *J. Mater. Sci. Mater. Electron.* **31**(6), 4503–4510 (2020)
101. T. Ohe, M. Kuribayashi, A. Tsuboi, K. Satori, M. Itabashi, K. Nomoto, Organic thin-film transistors with phase separation of polymer-blend small-molecule semiconductors: dependence on molecular weight and types of polymer. *Appl. Phys. Express* (2009). <https://doi.org/10.1143/APEX.2.121502>
102. T. Ohe, M. Kuribayashi, R. Yasuda, A. Tsuboi, K. Nomoto, K. Satori, M. Itabashi, J. Kasahara, Solution-processed organic thin-film transistors with vertical nanophase separation. *Appl. Phys. Lett.* **93**(5), 053303 (2008)
103. W.H. Lee, J.A. Lim, D. Kwak, J.H. Cho, H.S. Lee, H.H. Choi, K. Cho, Semiconductor–dielectric blends: a facile all solution route to flexible all-organic transistors. *Adv. Mater.* **21**(42), 4243–4248 (2009)
104. L. Zhang, D. Yang, Y. Wang, H. Wang, T. Song, C. Fu, S. Yang, J. Wei, R. Liu, B. Zou, Performance enhancement of FET-based photodetector by blending P3HT With PMMA. *IEEE Photonics Technol. Lett.* **27**(14), 1535–1538 (2015)
105. L. Qiu, J.A. Lim, X. Wang, W.H. Lee, M. Hwang, K. Cho, Versatile use of vertical-phase-separation-induced bilayer structures in organic thin-film transistors. *Adv. Mater.* **20**(6), 1141–1145 (2008)
106. P.S. Jo, D.T. Duong, J. Park, R. Sinclair, A. Salleo, Control of rubrene polymorphs via polymer binders: applications in organic field-effect transistors. *Chem. Mater.* **27**(11), 3979–3987 (2015)
107. L.Z. Qiu, X. Wang, W.H. Lee, J.A. Lim, J.S. Kim, D. Kwak, K. Cho, Organic thin-film transistors based on blends of poly(3-hexylthiophene) and polystyrene with a solubility-induced low percolation threshold. *Chem. Mater.* **21**(19), 4380–4386 (2009)
108. H.J. Jung, Y.J. Shin, Y.J. Park, S.C. Yoon, D.H. Choi, C. Park, Ultrathin, organic, semiconductor/polymer blends by scanning corona-discharge coating for high-performance organic thin-film transistors. *Adv. Funct. Mater.* **20**(17), 2903–2910 (2010)
109. Z. He, D. Li, D.K. Hensley, A.J. Rondinone, J. Chen, Switching phase separation mode by varying the hydrophobicity of polymer additives in solution-processed semiconducting small-molecule/polymer blends. *Appl. Phys. Lett.* **103**(11), 113301 (2013)
110. Z. He, Z. Zhang, K. Asare-Yeboah, S. Bi, Poly( $\alpha$ -methylstyrene) polymer and small-molecule semiconductor blend with reduced crystal misorientation for organic thin film transistors. *J. Mater. Sci. Mater. Electron.* **30**, 14335–14343 (2019)
111. Z. He, J. Chen, Z. Sun, G. Szulczewski, D. Li, Air-flow navigated crystal growth for TIPS pentacene-based organic thin-film transistors. *Org. Electron.* **13**(10), 1819–1826 (2012)
112. K. Asare-Yeboah, S. Bi, Z. He, D. Li, Temperature gradient controlled crystal growth from TIPS pentacene–poly( $\alpha$ -methyl styrene) blends for improving performance of organic thin film transistors. *Org. Electron.* **32**, 195–199 (2016)
113. K. Sim, A.K. Palai, G. Tarsoly, H. Na, S. Pyo, Polymer binder assisted, solution processed cyanophenyl functionalized diketopyrrolopyrrole microwire for n-channel field-effect transistors. *Synth. Met.* **250**, 152–160 (2019)
114. D.K. Hwang, C. Fuentes-Hernandez, J.D. Berrigan, Y.N. Fang, J. Kim, W.J. Potscavage, H. Cheun, K.H. Sandhage, B. Kippelen, Solvent and polymer matrix effects on TIPS-pentacene/polymer blend organic field-effect transistors. *J. Mater. Chem.* **22**(12), 5531–5537 (2012)
115. B.K.C. Kjellander, W.T.T. Smaal, J.E. Anthony, G.H. Gelinck, Inkjet printing of TIPS-PEN on soluble polymer insulating films: a route to high-performance thin-film transistors. *Adv. Mater.* **22**(41), 4612–4616 (2010)
116. L.-H. Chou, W.-C. Chang, G.-Y. He, Y.-C. Chiu, C.-L. Liu, Controllable electrical performance of spray-coated semiconducting small molecule/insulating polymer blend thin film for organic field effect transistors application. *React. Funct. Polym.* **108**, 130–136 (2016)
117. I. Bae, S.K. Hwang, R.H. Kim, S.J. Kang, C. Park, Wafer-scale arrays of nonvolatile polymer memories with microprinted semiconducting small molecule/polymer blends. *ACS Appl. Mater. Interfaces* **5**(21), 10696–10704 (2013)



118. N.L. Vaklev, R. Muller, B.V.O. Muir, D.T. James, R. Pretot, P. van der Schaaf, J. Genoe, J.S. Kim, J.H.G. Steinke, A.J. Campbell, High-performance flexible bottom-gate organic field-effect transistors with gravure printed thin organic dielectric. *Adv. Mater. Interfaces* **1**(3), 1300123 (2014)
119. Y.S. Chung, N. Shin, J. Kang, Y. Jo, V.M. Prabhu, S.K. Satija, R.J. Kline, D.M. DeLongchamp, M.F. Toney, M.A. Loth, B. Purushothaman, J.E. Anthony, D.Y. Yoon, Zone-refinement effect in small molecule–polymer blend semiconductors for organic thin-film transistors. *JACS* **133**(3), 412–415 (2011)
120. M.R. Niazi, R. Li, M. Abdelsamie, K. Zhao, D.H. Anjum, M.M. Payne, J. Anthony, D.-M. Smilgies, A. Amassian, Contact-induced nucleation in high-performance bottom-contact organic thin film transistors manufactured by large-area compatible solution processing. *Adv. Funct. Mater.* **26**(14), 2371–2378 (2016)
121. W. He, W. Xu, H. He, X. Jing, C. Liu, J. Feng, C. Luo, Z. Fan, S. Wu, J. Gao, G. Zhou, X. Lu, J. Liu, From unipolar, WORM-type to ambipolar, bistable organic electret memory device by controlling minority lateral transport. *Adv. Electron. Mater.* **6**(4), 1901320 (2020)
122. W.C. Xu, H.X. He, X.S. Jing, S.J. Wu, Z. Zhang, J.W. Gao, X.S. Gao, G.F. Zhou, X.B. Lu, J.M. Liu, High performance organic nonvolatile memory transistors based on HfO<sub>2</sub> and poly( $\alpha$ -methylstyrene) electret hybrid charge-trapping layers. *Appl. Phys. Lett.* **111**(6), 063302 (2017)
123. J.I. Han, C.-Y. Lim, S.K. Park, Y.-H. Kim, High-performance 2,8-difluoro-5,11-bis(triethylsilylethynyl) anthradithiophene thin-film transistors facilitated by predeposited ink-jet blending. *Jpn. J. Appl. Phys.* **52**(3R), 031601 (2013)
124. N. Shin, J. Kang, L.J. Richter, V.M. Prabhu, R.J. Kline, D.A. Fischer, D.M. DeLongchamp, M.F. Toney, S.K. Satija, D.J. Gundlach, B. Purushothaman, J.E. Anthony, D.Y. Yoon, Vertically segregated structure and properties of small molecule-polymer blend semiconductors for organic thin-film transistors. *Adv. Funct. Mater.* **23**(3), 366–376 (2013)
125. H.L. Zhong, J. Smith, S. Rossbauer, A.J.P. White, T.D. Anthopoulos, M. Heeney, Air-stable and high-mobility n-channel organic transistors based on small-molecule/polymer semiconducting blends. *Adv. Mater.* **24**(24), 3205–3211 (2012)
126. Z. He, Z. Zhang, K. Asare-Yeboah, S. Bi, J. Chen, D. Li, Polyferrocenylsilane semicrystalline polymer additive for solution-processed p-channel organic thin film transistors. *Polymers* **13**(3), 402 (2021)

**Publisher's Note** Springer Nature remains neutral with regard to jurisdictional claims in published maps and institutional affiliations.